

# Chapter 7

## The Biogeochemical Context of Marine Planktonic Ecosystems



**Teodoro Ramírez, María Muñoz, Andreas Reul, M. Carmen García-Martínez, Francina Moya, Manuel Vargas-Yáñez, and Begoña Bautista**

### 7.1 Introduction

#### 7.1.1 *Biogeochemistry and Phytoplankton Productivity of the Alboran Sea*

Although the Mediterranean Sea is considered in general an oligotrophic basin (Béthoux et al. 2002; D’Ortenzio and Ribera d’Alcalà 2009), it is able to sustain moderate levels of primary production. This fact is known as the “Mediterranean paradox” (Sournia 1973; Estrada 1996) which seems to be related to high levels of regenerated production and the existence of different fertilization mechanisms that inject nutrients into the euphotic layer. In fact, there are large differences in productivity between the different regions in the Mediterranean Sea, so that some areas are mesotrophic rather than oligotrophic (Stambler 2014). In these areas, primary production is considerably higher than the average for the whole Mediterranean basin (Bosc et al. 2004). In particular, the Alboran Sea is considered the most productive basin of the Mediterranean Sea (Bosc et al. 2004; Lazzari et al. 2012).

However, the Alboran Sea presents a high spatio-temporal variability in its hydrological and biogeochemical features as well as in its primary production. The enhanced productivity of the Alboran Sea, in comparison with other regions within

---

T. Ramírez · M. Muñoz · M. C. García-Martínez · F. Moya · M. Vargas-Yáñez  
Instituto Español de Oceanografía, Centro Oceanográfico de Málaga, Fuengirola (Málaga),  
Spain  
e-mail: [teodoro.ramirez@ieo.es](mailto:teodoro.ramirez@ieo.es); [maria.munoz@ieo.es](mailto:maria.munoz@ieo.es); [mcarmen.garcia@ieo.es](mailto:mcarmen.garcia@ieo.es);  
[francina.moya@ieo.es](mailto:francina.moya@ieo.es); [manolo.vargas@ieo.es](mailto:manolo.vargas@ieo.es)

A. Reul · B. Bautista (✉)  
Departamento de Ecología y Geología, Facultad de Ciencias, Universidad de Málaga, Málaga,  
Spain  
e-mail: [areul@uma.es](mailto:areul@uma.es); [bbautista@uma.es](mailto:bbautista@uma.es)

the Mediterranean, is due to different periodic and recurrent fertilization mechanisms operating in the Strait of Gibraltar and also within the Alboran Sea, which are addressed and discussed in this chapter. These fertilization processes lead to the injection of new nutrients from subsurface waters into the euphotic layer supporting enhanced phytoplankton biomass and primary production, particularly in the North-western (NW) Alboran Sea (Minas et al. 1991; Garcia-Gorriz and Carr 2001; Bosc et al. 2004; Reul et al. 2005; Macías et al. 2007). However, the biogeochemical signatures of the upwelled waters at the Strait of Gibraltar and its proximities, and also those of Atlantic waters masses incursions, are progressively lost during the progress of these waters through the Alboran Sea. As the distance to the Strait increases the upper waters of the Alboran Sea become more oligotrophic (Bosc et al. 2004) due to the uptake of nutrients by phytoplankton and also to a lower number of fertilization mechanisms and to a higher variability in the eastern sector (Ramírez 2007; Renault et al. 2012; Oguz et al. 2014).

This chapter reviews the biogeochemical features of the different water masses found in the Alboran Sea, the different fertilization mechanisms (from upwelling events to incursions of nutrient-rich North Atlantic Deep Water NACW) which promote the injection of nutrient into the photic layer. The chapter also examines the nutrient dynamics in this basin and the potential limitation of phytoplankton by nutrients, as evidenced from the molar nitrate:phosphate (N:P) and nitrate:silicate (N:Si) ratios, and discusses the role of phytoplankton uptake in regulating nutrient concentrations and molar ratios in this basin. In addition, it also addresses the distribution patterns of chlorophyll-a (Chl-a) and primary production (PP) in relation to the hydrology and biogeochemical fields. The last section of this chapter analyses the effects of climate change and ocean acidification on the biogeochemistry and primary production in the Mediterranean and the Alboran Sea.

The average vertical profiles (annual climatologies) of nutrients and dissolved oxygen, as well as the average seasonal vertical profiles (seasonal climatologies) of Chl-a in the Alboran Sea (Manca et al. 2004) were plotted using data provided by OGS Istituto Nazionale di Oceanografia e Geofisica Sperimentale. Source: Data and metadata are provided by the Italian National Oceanographic Data Center of the OGS Istituto Nazionale di Oceanografia e Geofisica Sperimentale (NODC/OGS), acting within the International Oceanographic Data Exchange System of the UNESCO Intergovernmental Oceanographic Commission (IOC) since 27/6/2002.

In order to illustrate the singularities of the Alboran Sea, in comparison with the rest of the Mediterranean Sea, as well as to show the high spatial variability of nitrate concentration, N:P molar ratio, Chl-a and PP in this basin, average integrated values for these variables have been obtained. The data were “Generated using E.U. Copernicus Marine Service Information.” Monthly mean data of Mediterranean Sea Biogeochemistry Reanalysis (Teruzzi et al. 2016) (Product: MEDSEA\_REANALYSIS\_BIO\_006\_008) ([https://doi.org/10.25423/MEDSEA\\_REANALYSIS\\_BIO\\_006\\_008](https://doi.org/10.25423/MEDSEA_REANALYSIS_BIO_006_008)) were downloaded from the E.U. Copernicus Marine Environment Monitoring Service website (<http://marine.copernicus.eu/services-portfolio/access-to-products>) and processed to get the average integrated values (0–100 m) over the period 1999–2016 for those variables in the Mediterranean

and the Alboran Sea. The processed data correspond to the month of May, one of the most productive months in the Alboran Sea (Lazzari et al. 2012).

On the other hand, the data on the nutrient distribution at 50 m depth in the Alboran Sea during the IctioAlboran 0793 survey (July 1993) were provided by Dr. Juan Pérez de Rubín (Instituto Español de Oceanografía, IEO).

## 7.2 Nutrients Dynamics: Coupling with Physical Processes

### 7.2.1 *Nutrients and Water Masses in the Alboran Sea*

Surface layers in the Alboran Sea are occupied by Surface Atlantic Water (SAW), known also as Modified Surface Atlantic Water (MSAW), which has its origin in the Gulf of Cadiz (see Chap. 5 of this book). Many studies have reported that the SAW entering the Alboran Sea is nutrient poor or even nutrient depleted (Minas et al. 1991; Béthoux et al. 1992; Turley 1999) due to the consumption by phytoplankton in the Gulf of Cadiz and the Strait of Gibraltar. However, the question of whether the Atlantic water entering into the Alboran Sea is depleted or not in nutrients has been matter of debate during the last decades (Béthoux et al. 1992; Dafner et al. 2003; Huertas et al. 2012). Much of these discrepancies could be due to the fact that in many studies nutrient concentrations have been reported for the Atlantic inflow entering into the Alboran Sea rather than for the SAW. At the Strait of Gibraltar, and due to intense mixing processes, the upwelling of subsurface rich nutrient Mediterranean waters into the Atlantic surface layer takes place. Other processes like incursions of NACW also occur (see below), thereby the nutrient load in the Atlantic inflow largely depends on these processes and also on the biological activity (Gómez et al. 2000). Moreover, mixing at the Strait is largely controlled by different physical factors (see Sect. 7.2.2). Therefore, nutrient levels in the Atlantic inflow can be rather variable. Nevertheless, the nutrient signatures of the SAW at the Strait have been obtained from the analysis of water masses (Minas et al. 1991; Gómez et al. 2000), where SAW is characterized by nitrate  $<2 \mu\text{M}$ , phosphate  $<0.01 \mu\text{M}$ , and silicate  $<1 \mu\text{M}$  (Gómez et al. 2000).

NACW has been detected by several studies in the upper layer of the Strait of Gibraltar and also in the Alboran Sea (Gascard and Richez 1985; Minas et al. 1991; Gómez et al. 2000; Ramírez et al. 2005; Ramírez-Romero et al. 2014). The entrance of this water mass into the Alboran Sea is strongly modulated by the tidal cycles at the Strait (see Sect. 7.2.2). NACW is a water mass rich in nutrients, with nitrate  $\sim 5\text{--}7 \mu\text{M}$ , phosphate  $\sim 0.35\text{--}0.45 \mu\text{M}$ , and silicate  $\sim 2\text{--}3 \mu\text{M}$  (Gómez et al. 2000). Although other studies have found lower phosphate concentrations ( $0.09 \mu\text{M}$ ) associated to this water mass at the Strait of Gibraltar (Ramírez-Romero et al. 2014).

On the other hand, the intermediate and deep water masses found in the Alboran Sea are Winter Intermediate Water (WIW), Levantine Intermediate Water (LIW), and Western Mediterranean Deep Water (WMDW) (see Chap. 5 of this book). These water masses are characterized by different biogeochemical signatures due to their

different origins and different residence times (Minas et al. 1991). During their progress from the Western Mediterranean towards the Alboran Sea, the biogeochemical properties of the intermediate and deep Mediterranean water masses are progressively modified by mixing with adjacent water masses, as well as by the accumulation of organic matter from the euphotic zone (by vertical flux or lateral advection) and bacterial activity (Minas et al. 1991).

The WIW is formed in winter in the NW Mediterranean (Salat and Font 1987; Millot 1999) and flows along the continental slope of the Iberian Peninsula (Vargas-Yáñez et al. 2012), reaching the Balearic Sea by spring (Pinot and Ganachaud 1999; Pinot et al. 2002) and the Alboran Sea by summer or beginning of autumn (Font 1987). Its recent origin, in comparison with other intermediate water masses, is reflected in its biogeochemical features. In the NW Mediterranean, its oxygen content is relatively high (Minas et al. 1991; Balbín et al. 2014) but it decreases progressively during its transit towards the Alboran Sea. In the Alboran Sea, there are very few data on the biogeochemical features of this water mass. Ramírez (2007) found a relative maximum of dissolved oxygen and a relative minimum of nutrient concentrations at 200 m depth, linked to a temperature minimum ( $\theta$ ) ranging from 13.09 °C to 13.20 °C at stations located at the border of the continental slope, where according to Parrilla and Kinder (1987) the WIW flows towards the Strait of Gibraltar. The presence of a temperature ( $\theta$ ) minimum was detected in summer and autumn at salinities ranging from ~37.90 to 38.30 (Ramírez 2007), while it was much less defined or even absent in winter and spring. At the  $\theta$  minimum the dissolved oxygen concentration was on average 202.88  $\mu\text{M}$ , while the mean nitrate, phosphate, and silicate concentrations were 6.55  $\mu\text{M}$ , 0.25  $\mu\text{M}$ , 3.75  $\mu\text{M}$ , respectively. All these findings suggest the presence of WIW, but  $\theta$  minimum values were higher than the typical  $\theta$  minimum associated to the WIW in the Alboran Sea (Parrilla and Kinder 1987), indicating a warmer WIW. This could be due to the high variability observed in the formation of this water mass and to the variability of its circulation in the Western Mediterranean (Pinot et al. 2002; Vargas-Yáñez et al. 2012), which affect the mixing with other water masses.

The most important intermediate water mass in the Alboran Sea is the LIW (Parrilla et al. 1986; Parrilla and Kinder 1987; Minas et al. 1991). After reaching the NW Mediterranean, this water mass flows towards the Alboran Sea along the continental slope below the WIW (Font 1987; Millot 1999). It has been suggested that due to this seasonality the greater volume of LIW arrives to the Alboran Sea by summer-early autumn (Font 1987). The thermohaline and geochemical signatures of LIW remain clearly distinctive when they enter into the Alboran Sea. Nevertheless, during its journey towards the Alboran Sea, the LIW mixes with WIW and Mediterranean deep waters (Parrilla and Kinder 1987) modifying its levels of dissolved oxygen. These levels are also modified by microbial respiration in the core of LIW (Minas et al. 1991). Thus when the LIW arrives to the Alboran Sea it presents lower dissolved oxygen levels and higher nutrients concentrations than in the NW Mediterranean (Minas et al. 1991). Averaged dissolved oxygen values in the LIW for the whole Alboran Sea have been estimated to be 4.21  $\text{ml}\cdot\text{l}^{-1}$  (Manca et al. 2004), although the lowest values are found in the Western Alboran basin (Minas et al.

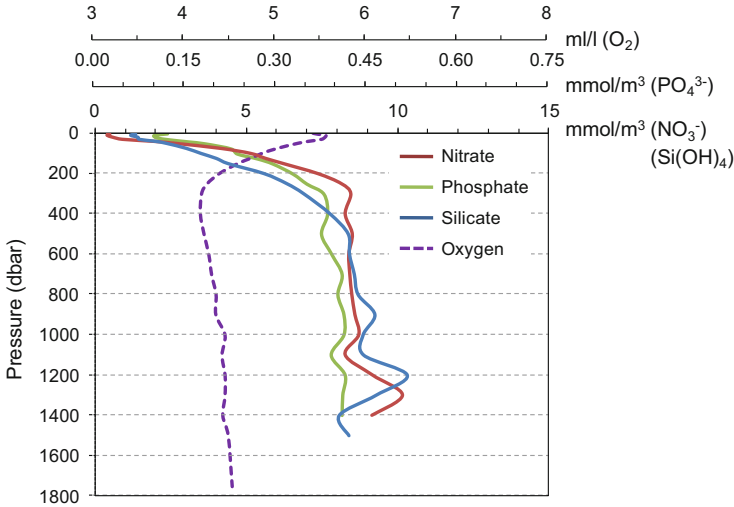


**Fig. 7.1** Average vertical profiles (annual climatologies) of inorganic nutrients and dissolved oxygen in the Alboran Sea (Manca et al. 2004). Source: Data and metadata are provided by the Italian National Oceanographic Data Center of the OGS Istituto Nazionale di Oceanografia e Geofisica Sperimentale (NODC/OGS), acting within the International Oceanographic Data Exchange System of the UNESCO Intergovernmental Oceanographic Commission (IOC) since 27/6/2002

1991; Balbín et al. 2014; García-Martínez et al. 2019), with values ranging from  $\sim 3.2$  to  $3.9 \text{ ml}\cdot\text{l}^{-1}$  (Balbín et al. 2014; García-Martínez et al. 2019). Manca et al. (2004) reported averaged nutrient values in the LIW layer for the whole Alboran basin, with concentrations of nitrate  $8.49 \mu\text{M}$ , phosphate  $0.37 \mu\text{M}$ , and silicate  $8.36 \mu\text{M}$ . Other studies have reported a maximum of nitrate and phosphate associated to the oxygen minimum in the Northern Alboran Sea (García-Martínez et al. 2019), which has been detected at depths  $\sim 300$  m and  $500$  m in the Western and the Eastern Alboran Sea, respectively, coinciding with the depth level of the LIW. The average concentrations at the nitrate maximum range from  $\sim 9 \mu\text{M}$  to  $11 \mu\text{M}$ , with lower values in autumn and higher in summer associated to the LIW in this sector of the Alboran (García-Martínez et al. 2019). However, former studies (Packard et al. 1988; Minas et al. 1991) did not find a nutrient maximum associated to the salinity maxima of the LIW (at  $\sim 400$  m depth) in the Western Alboran Sea. The average vertical profiles for nitrate, phosphate, silicate, and dissolved oxygen for the Alboran Sea (annual climatologies) are shown in Fig. 7.1.

Below the LIW layer, denser less saline, and colder WMDW is found occupying the deepest part of the Alboran Sea basin (Parrilla and Kinder 1987; Minas et al. 1991; Manca et al. 2004). The WMDW is formed in winter in the Gulf of Lions (Millot 1999) and flows towards the Alboran Sea (see Chap. 5 of this book). Due to its recent origin, the WMDW is characterized by higher dissolved oxygen levels than the LIW (Minas et al. 1991). Thus in the NW Mediterranean Sea dissolved oxygen concentrations of this deep water mass are  $\sim 4.6\text{--}4.7 \text{ ml}\cdot\text{l}^{-1}$  (Minas et al. 1991).

According to its recent origin, the WMDW should also have lower nutrient concentrations than intermediate waters. In accordance Béthoux et al. (1998) reported a weak maximum for nitrate and phosphate in the Western Mediterranean associated to intermediate waters, with averaged salinity  $\geq 38.492$ , and slightly lower nitrate and phosphate concentrations in deep waters. Similar profiles have been reported by other authors in the NW Mediterranean (e.g., Karafistan et al. 2002). In contrast silicate concentrations found in deep Mediterranean waters were slightly higher compared to intermediate waters, which has been attributed to the slower remineralization rates of silicate relative to nitrate and phosphate (Béthoux et al. 1998). However other studies have found that nutrient concentrations associated to deep Mediterranean waters in the NW Mediterranean, as well as in the Alboran Sea, are slightly higher than the concentrations found in the LIW (Manca et al. 2004). These abnormally high nutrient concentrations in the NW Mediterranean have been attributed to an increase of nutrient inputs from terrestrial and atmospheric sources (Manca et al. 2004). During its transit from the Gulf Lions towards the Alboran Sea the WMDW loses part of its biogeochemical signatures. In the Alboran Sea, the average dissolved oxygen concentration associated to this water mass is  $4.50 \text{ ml}\cdot\text{l}^{-1}$  (Manca et al. 2004). This value is similar to values reported in earlier studies (Minas et al. 1991) in the Western Alboran Sea. The average nitrate and phosphate concentrations in the WMDW for the Alboran basin have been estimated to be  $9.13 \text{ }\mu\text{M}$  and  $0.41 \text{ }\mu\text{M}$  respectively (Manca et al. 2004), while the average silicate concentration associated to WMDW in the Alboran Sea was  $8.38 \text{ }\mu\text{M}$  (Manca et al. 2004) (i.e., similar to the value found by these authors for the LIW in this basin). In the Western Alboran Sea Minas et al. (1991) detected the higher silicate concentrations in the WMDW, with values  $\sim 10 \text{ }\mu\text{M}$  on the African continental slope, due to the lifting of this deep water mass along the southern continental slope, while nitrate in deep waters was uniform with values  $\sim 9.0 \text{ }\mu\text{M}$ .

### ***7.2.2 Fertilization Mechanisms: Sources of New Nutrients to the Photic Layer***

The most productive areas in the Alboran Sea are found in its NW sector, in particular on the Iberian continental margin between Europa Point and Marbella as well as in the proximities of the Strait of Gibraltar and the northern part of the Western Anticyclonic Gyre (WAG) (Minas et al. 1991; Baldacci et al. 2001; Reul et al. 2005). The enhanced productivity in this area, which is clearly distinguishable from satellite images (García-Gorrioz and Carr 1999, 2001), is caused by different fertilization mechanisms that induce the upwelling of colder subsurface nutrient-rich waters and promote phytoplankton blooms (Minas et al. 1991; Sarhan et al. 2000; Reul et al. 2005; Ramírez et al. 2005). The presence of cold surface waters in this area is almost permanent (Renault et al. 2012) and is favored by the bottom topography of the continental margin in the NW Alboran Sea, where the existence

of submarine canyons could play a role in the exchange of waters between the continental shelf and deep waters (Parrilla et al. 1986; Lafuente et al. 1999; Sarhan et al. 2000). On the other hand, in the Alboran Sea, the intermediate Mediterranean waters flow following the geometry of the north continental shelf, banking against the slope (Parrilla et al. 1986) which facilitates its upwelling.

By far one of the most important fertilization mechanisms, due to its effect along all the northern continental shelf of the Alboran Sea (from Europa Point to further East of Cape Gata), is the upwelling induced by westerlies (Sarhan et al. 2000; Baldacci et al. 2001; Garcia-Gorriz and Carr 1999, 2001; Bakun and Agostini 2001; Mercado et al. 2012). Wind-driven upwelling is particularly important in coastal and continental shelf waters (Sarhan et al. 2000). This type of upwelling is more intense in spring coinciding with stronger westerlies (Garcia-Gorriz and Carr 1999, 2001; Ramírez et al. 2005). Thus the wind regime has important consequences on the Chl-*a* variability throughout the year. In the NW Alboran Sea, it has been reported that on average 70% of nitrate and 83% of silicate temporal variability (Ramírez 2007) was explained by the average seasonal zonal wind (E-W) component and seawater temperature, over 12 seasonal cruises, using multiple regression model. Under certain conditions, the upwelling can be attenuated or even inhibited by different factors. Thus the presence of the Atlantic jet close to the Spanish coast may hamper the upwelling of subsurface waters, caused by Ekman pumping due to westerlies (Sarhan et al. 2000). On the African continental shelf, westerlies induce downwelling of poor nutrient surface waters hampering phytoplankton growth (Bakun and Agostini 2001). On the other hand, easterlies cause convergence and downwelling of surface waters along the Spanish coast, while they produce upwelling along the African coast. During summer and autumn, when easterlies dominate the wind regime, downwelling occurs along the Spanish coast and upwelling takes place along the African coast (Bakun and Agostini 2001; Stanichny et al. 2005). The presence of a marked thermocline from July to September can also hamper the upwelling (Garcia-Gorriz and Carr 2001). Nevertheless, upwelling phenomena can occur even in summer under strong favorable winds, leading to occasional blooms (Ramírez 2007).

In addition to wind-driven upwelling, in this sector of the Alboran Sea, the path of Atlantic jet leads to the formation of an intense geostrophic front located at the northernmost limit of the WAG (Minas et al. 1991; Vargas-Yañez et al. 2002; Garcia-Gorriz and Carr 2001; Vélez-Belchí et al. 2005). The instabilities and vertical velocities associated to the ageostrophic cross-frontal circulation promote the continuous vertical supply of nutrients to the photic zone (Tintoré et al. 1991; Gil and Gomis 1994; Sarhan et al. 2000). Another fertilization mechanism is linked to the variability of the Atlantic jet in the Western Alboran Sea. The position of the jet show fluctuations over time caused by variations in both the inflow of Atlantic water and the entrance angle of the Atlantic jet into the Alboran Sea (Sarhan et al. 2000; Vargas-Yañez et al. 2002). Thus the jet can shift southwards several km in short time periods (2–3 days) (Sarhan et al. 2000; Reul et al. 2005) leading to the upwelling of subsurface waters north of the jet. This upwelling mechanism seems only to occur

during the southward shift of the jet, and its intensity is low compared to upwelling by westerlies (Sarhan et al. 2000).

Lateral advection of surface nutrient-rich waters by the main Atlantic current has also been described as an important fertilization mechanism in the Western Alboran Sea, as well as for other areas located at the center of the basin (Minas et al. 1991; Garcia-Gorriz and Carr 2001; Ruiz et al. 2001). These surface nutrients rich waters have their origin in upwelling events at the Strait of Gibraltar as well as in coastal upwelling occurring between Europa Point and Marbella (Minas et al. 1991; Garcia-Gorriz and Carr 2001; Baldacci et al. 2001; Oguz et al. 2014). Other studies have also pointed to the advection of phytoplankton rich waters from the Gulf of Cadiz towards the Alboran Sea as a source of phytoplankton biomass (Navarro et al. 2011; Ramírez-Romero et al. 2014). In the Alboran Sea, the surface waters are advected further east by the Atlantic jet following the main circulation pattern (Baldacci et al. 2001; Ruiz et al. 2001; Garcia-Gorriz and Carr 2001; Sánchez-Vidal et al. 2004), being an important source of nutrients and phytoplankton to the central and eastern part of the basin.

The upwelling Mediterranean waters at the Strait of Gibraltar is caused by different processes (Minas et al. 1991; Gómez et al. 2000; Echevarría et al. 2002) involving intense mixing and entrainment between nutrient-rich Mediterranean waters and Atlantic waters. These mixing processes are governed by the exchange of water masses at the Strait, which largely depend on the tidal cycles and the bottom topography (Echevarría et al. 2002). Dafner et al. (2003) calculated that ~16% of Mediterranean water outflow entrains with the Atlantic inflow and recirculates back into the Alboran Sea. Other studies have estimated that the mixing process during spring tides, alongside with injection of waters from coastal areas in the Gulf of Cadiz, would account for 31% of the total nitrate supply to the Alboran Sea through the Strait, while upwelling due to internal waves would account for 74% of the total entry of phosphate in the Alboran Sea (Ramírez-Romero et al. 2014). The upwelled waters at the Strait are advected towards the Alboran Sea by the Atlantic inflow. As indicated above, internal waves generated at the Camarinal Sill play a major role in the mixing processes at the Strait particularly during spring tides (Gascard and Richez 1985; Echevarría et al. 2002; Vázquez et al. 2008). In addition, it has been suggested that the trapping of internal waves at the Camarinal Sill could increase the mixing (Bruno et al. 2002). Once the train of waves enters into the Alboran Sea their path produces the intermittent lifting of subsurface waters (Vázquez et al. 2009; Van Haren 2014) leading to the pulsed injection of nutrients into the upper layer.

The nutrient enrichment of surface waters in the Western Alboran Sea is also caused by incursions of nutrient-rich NACW in the Atlantic inflow at the Strait of Gibraltar (Minas et al. 1991; Gómez et al. 2000, 2001; Ramírez-Romero et al. 2014), which are controlled by tidal cycles. The incursions of large amounts of NACW occur at spring tides, while at neap tides the incursions of NACW are discontinuous (Gómez et al. 2004; Ramírez-Romero et al. 2014). Once these incursions of NACW have reached the upper layers they are advected by the Atlantic inflow into the Alboran Sea and mixed with the surface waters (Minas et al. 1991; Echevarría et al. 2002), contributing to the fertilization of the euphotic layer in the western sector of



this basin. During neap tides and in absence of internal waves the Atlantic inflow accounts for 69% of nitrate inputs to the Mediterranean from the Atlantic, mostly due to the contribution of NACW (Ramírez-Romero et al. 2014).

The presence of submesoscale cyclonic eddies in the North Alboran Sea (from Estepona to Cape Gata) has also been reported by a number of papers as a relevant source of new nutrients to the photic layer (Sarhan et al. 2000; Reul et al. 2005; Ramírez et al. 2005; García-Martínez et al. 2019). These eddies are formed from filaments detached from the main Atlantic current and they can persist for several days (Parrilla and Kinder 1987; Ramírez et al. 2005; Reul et al. 2005; García-Martínez et al. 2019). One of the most recurrent cyclonic cell is found off Estepona (e.g., Parrilla and Kinder 1987; Perkins et al. 1990; Cano and García Lafuente 1991; Baldacci et al. 2001) whose formation seems to be linked to the southward shift of the jet (Sarhan et al. 2000).

In the eastern sector of the Alboran Sea, the ageostrophic cross-frontal circulation associated to the presence of an almost permanent geostrophic front, caused by the path of the Atlantic jet, is one of the main fertilization mechanisms in this eastern sector. The front is known as the “Almeria-Oran front” and it separates the less saline and colder SAW in the Alboran basin from saltier and warmer Surface Mediterranean Waters (SMW) found in the Algero-Balear Basin (Tintoré et al. 1991; Prieur and Sournia 1994). The front exhibits a high variability linked to the high mesoscale instabilities in the general circulation pattern in the eastern basin compared to the western one (Millot 1999; Prieur and Sournia 1994; Renault et al. 2012). When the Eastern Anticyclonic Gyre (EAG) is well developed, usually in summer and autumn, the front is found at the easternmost boundary of this gyre (Prieur and Sournia 1994). However in winter the EAG is usually absent (Viúdez et al. 1996; Vargas-Yañez et al. 2002; Snaith et al. 2003) and the Atlantic jet shifts southwards and flows closer to the African coast (Claustre et al. 1994; Prieur and Sournia 1994; Renault et al. 2012).

### ***7.2.3 Distribution Patterns of Inorganic Nutrients (N, P, and Si)***

The dynamics of inorganic nutrients in the Alboran Sea presents a high spatial and temporal variability as a result of the high hydrodynamic variability and to the intense biological productivity in this basin. As a result, steeped nutrient gradients are observed both in the vertical and horizontal distribution (Figs. 7.1 and 7.2). The lowest nutrient concentrations in the Alboran Sea are usually found and the center of the WAG and the EAG (Fig. 7.2). Both gyres are downwelling zones where SAW, impoverished in nutrient due to the previous consumption by phytoplankton, converges, and sinks (Parrilla and Kinder 1987). Consequently, nutrient concentrations in the Alboran Sea central areas are particularly low during the stratification period, being frequently  $<0.25 \mu\text{M}$  for nitrate,  $<0.06 \mu\text{M}$  for phosphate, and  $<0.70 \mu\text{M}$  for

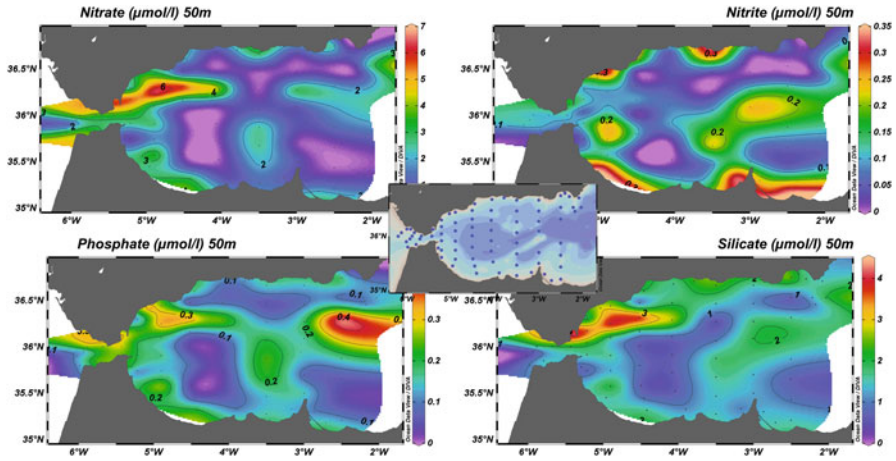


**Fig. 7.2** Nitrate, nitrite, phosphate, and silicate concentration ( $\mu\text{mol}\cdot\text{l}^{-1}$ ) at 50 m depth during IctioAlboran93 survey conducted in July 1993 by IEO. The stations are shown in the map at the center of the figure [Source: Figure based on data provided by Dr. Juan Pérez de Rubín (IEO)]

silicate (Gil and Gomis 1994; Rubín et al. 1992, 1997; Cano et al. 1997). Other studies have reported also low concentrations in areas of the continental margin of the NW Alboran Sea during the stratification period, with nitrate and sometimes phosphate below their detection limit above the thermocline, while silicate concentrations remained above  $0.8 \mu\text{M}$  (Ramírez et al. 2005; Ramírez 2007). Likewise, very low nutrient concentrations have also been found usually in adjacent areas north and east of the EAG due to the presence of warmer, saltier, and nutrient-poor MSW coming from the Algero-Balear basin. In the Mediterranean waters adjacent to the Almeria-Oran front phosphate concentrations in the upper 20 m are frequently below the detection limit (Jacquet et al. 2002; Leblanc et al. 2004), while nitrate and silicate are low but detectable with the lower concentrations around  $0.03\text{--}0.06 \mu\text{M}$  and  $0.8 \mu\text{M}$ , respectively (Leblanc et al. 2004). In contrast, the highest nutrient concentrations in the Alboran Sea are usually found at the vicinities of the Strait of Gibraltar and along the NW sector of the Spanish continental margin, where intense upwelling induced by different mechanisms takes place very frequently throughout the year (Minas et al. 1991; Baldacci et al. 2001; Renault et al. 2012). Thus, at the eastern side of the Strait of Gibraltar nitrate concentrations as high as  $\sim 5.0 \mu\text{M}$  have been found in the Atlantic waters, while phosphate concentration can reach values around  $\sim 0.30 \mu\text{M}$  and silicate up to  $\sim 3.0 \mu\text{M}$  (Gómez et al. 2000; Dafner et al. 2003; Huertas et al. 2012). Nevertheless, the variability at the Strait is very high and other authors have reported lower concentrations (e.g., Gómez et al. 2001; Echevarría et al. 2002; Ramírez-Romero et al. 2014). The variability of nutrients in this area depends on the tidal cycle, water exchange, stratification of the water column, the occurrence of mixing events, the incursions of NACW, and the wind

forcing (Gómez et al. 2000; Echevarría et al. 2002). On the continental margin of the NW Alboran Sea, the highest nutrient concentrations are detected during intense coastal upwelling events (Gil and Gomis 1994; Prieto et al. 1999; Ramírez et al. 2005; Reul et al. 2005; Ramírez 2007; Macías et al. 2008; Mercado et al. 2012). Wind-driven upwelling events normally lead to nitrate concentrations around 2.0–3.0  $\mu\text{M}$  in the upper 20 m of the water column on the continental margin, while phosphate and silicate concentrations are frequently around 0.15–0.20  $\mu\text{M}$  and 1.5–2.0  $\mu\text{M}$ , respectively (Ramírez et al. 2005; Reul et al. 2005; Mercado et al. 2014). Similar nutrient concentrations have also been found at the geostrophic front associated to the path of Atlantic jet in this area (Morán and Estrada 2001; Arin et al. 2002; Reul et al. 2005; Mercado et al. 2014). Wind-driven upwelling events frequently take place between November–March (García-Gorriz and Carr 2001), but they may sporadically occur throughout all year, thereby similarly high nutrient concentrations in the upper layers have been occasionally reported in the NW Alboran Sea during late spring (June) and the stratification period (e.g., Rubín et al. 1999; Prieto et al. 1999; Ramírez 2007; Lazzari et al. 2012). Nevertheless, during the non-bloom period, which extends from May to September (García-Gorriz and Carr 2001), coastal upwellings are less frequent and nutrient concentrations at the surface tend to decline. However, the fertilizing effect associated to the front persists even during the stratification period (García-Gorriz and Carr 2001). Thus nitrate concentrations in the frontal area during the stratification period are  $>2.0 \mu\text{M}$ , while north and south of the jet they are  $<0.5 \mu\text{M}$  (Reul et al. 2005).

As a consequence of the contrasting oceanographic conditions between coastal and offshore waters, sharp coastal-offshore nutrient gradients are frequently observed in the NW Alboran Sea (e.g., Gil and Gomis 1994; Rubín et al. 1997, 1999; Prieto et al. 1999; García-Gorriz and Carr 2001; Mercado et al. 2014) (Fig. 7.2). In addition in the continental margin around 4.5° W there is usually a marked difference between the waters under the influence of the front associated to the Atlantic jet and the waters on the continental margin located north-northeast of the jet (Fig. 7.2), out of the influence of the jet. Thus, the general circulation pattern explains the relatively lower nutrient concentrations found in areas of the northern continental margin of the Alboran Sea located northeast of the jet, as observed in Fig. 7.2, in comparison with areas under the direct influence of the front associated to the Atlantic jet (Gil and Gomis 1994; Ramírez 2007).

Nevertheless, it has to be highlighted that the presence of circulation cells between Malaga and Motril is relatively frequent, with alternation of upwelling and downwelling (Gil and Gomis 1994). Thus, relatively high nutrient concentrations on the continental shelf in the area off Cape Sacatraf (close to Motril) are frequently found (Gil and Gomis 1994; García-Martínez et al. 2019), due to the recurrence in this area of a cyclonic eddy (Parrilla and Kinder 1987; Baldacci et al. 2001). On the other hand, several studies have reported an eastward decline of nutrients in the Alboran Sea (e.g., Denis-Karafistan et al. 1998; Karafistan et al. 2002). On the north continental margin, the lower concentrations have been observed in Cape Gata (García-Martínez et al. 2019). Nevertheless, nutrients in the frontal area of the Almería-Oran front are high compared to adjacent waters

(Fig. 7.2) (Bianchi et al. 1994; Claustre et al. 1994; Leblanc et al. 2004). Gil and Gomis (1994) detected very high nitrate concentration  $>6.5 \mu\text{M}$  at 50 m in offshore waters off the Almeria Bay, associated to a strong salinity gradient. Lower nitrate concentrations were found by Bianchi et al. (1994) at 50 m in the frontal area ( $\sim 3 \mu\text{M}$  nitrate), while according to Leblanc et al. (2004) nitrate was  $\sim 1\text{--}2 \mu\text{M}$  at 50 m depth in the Almeria-Oran front area. Figure 7.3b shows the climatology of the depth-integrated nitrate concentration in the upper 100 m during the month of May (spring), one of the most productive months in the Alboran Sea (Lazzari et al. 2012). A marked north to south nitrate gradient in the Alboran Sea can be observed, with higher concentrations in the Northern Alboran coasts and the lower values observed in the Southern Alboran coasts (Fig. 7.3b). These marked differences are due to the convergence of nutrient-poor Atlantic waters in the southern part, while in the northern part the frequent upwellings lead to much higher concentrations.

In general, the vertical distribution of nutrients in the Alboran Sea follows a typical vertical pattern with low concentrations in surface waters and below a marked nutricline, that extends to depths around 250–300 m (Minas et al. 1991; Béthoux et al. 1992) (Fig. 7.1). The marked nutricline reflects the influence of Mediterranean waters below the nutrient-poor SAW layer (Minas et al. 1991). In the Western Alboran Sea, below the nutricline nitrate concentrations remains nearly constant ( $\sim 9.0 \mu\text{M}$ ) while phosphate concentration ranges between  $\sim 0.45$  and  $0.50 \mu\text{M}$ . In contrast, silicate concentration continues increasing more slowly below the nutricline, reaching its higher values ( $\sim 10 \mu\text{M}$ ) at the bottom of the basin in the Western Alboran Sea (Minas et al. 1991). However in areas close to the Strait of Gibraltar, where the presence of a oxygen extraminimum has been reported (Packard et al. 1988; Minas et al. 1991), the vertical profiles of nitrate and phosphate present a weak maximum at the lower limit of the nutricline (200–250 m), which is more conspicuous for nitrate (Minas et al. 1991). The maximum coincides with a dissolved oxygen extraminimum in the water column, where concentrations as low as  $3.8 \text{ ml}\cdot\text{l}^{-1}$  are reached (Packard et al. 1988; Minas et al. 1991). This extraminimum and the associated nitrate and phosphate maximum are the consequence of the intense export of organic matter from the nearby high productive areas in the NW Alboran Sea towards the center of the WAG, where the organic matter accumulates and sink promoting the growth of bacterial communities and the respiration of the accumulated organic matter, leading to the oxygen extraminimum and to the nutrient maxima (Minas et al. 1991).

At the center of the WAG and the EAG the subduction of SAW causes a pronounced deepening of the 37.5 isohaline, which is considered the interface between Atlantic and Mediterranean waters in this basin (Parrilla and Kinder 1987). As a result, a thick SAW layer ( $\sim 150\text{--}200$  m depth) is found at the center of both gyres (Lafuente et al. 1998; Leblanc et al. 2004). The downwelling of poor nutrient SAW at the center of both gyres is reflected in the nutricline, which reaches its deepest locations at the core of both anticyclonic gyres. Accordingly, the nitracline has been found at depths ranging from  $\sim 70$  to 115 m at the center of the anticyclonic gyres (Leblanc et al. 2004; Morán and Estrada 2001; Mercado et al. 2014), and the phosphacline has been found a depths varying from  $\sim 50$  to  $\sim 170$  m

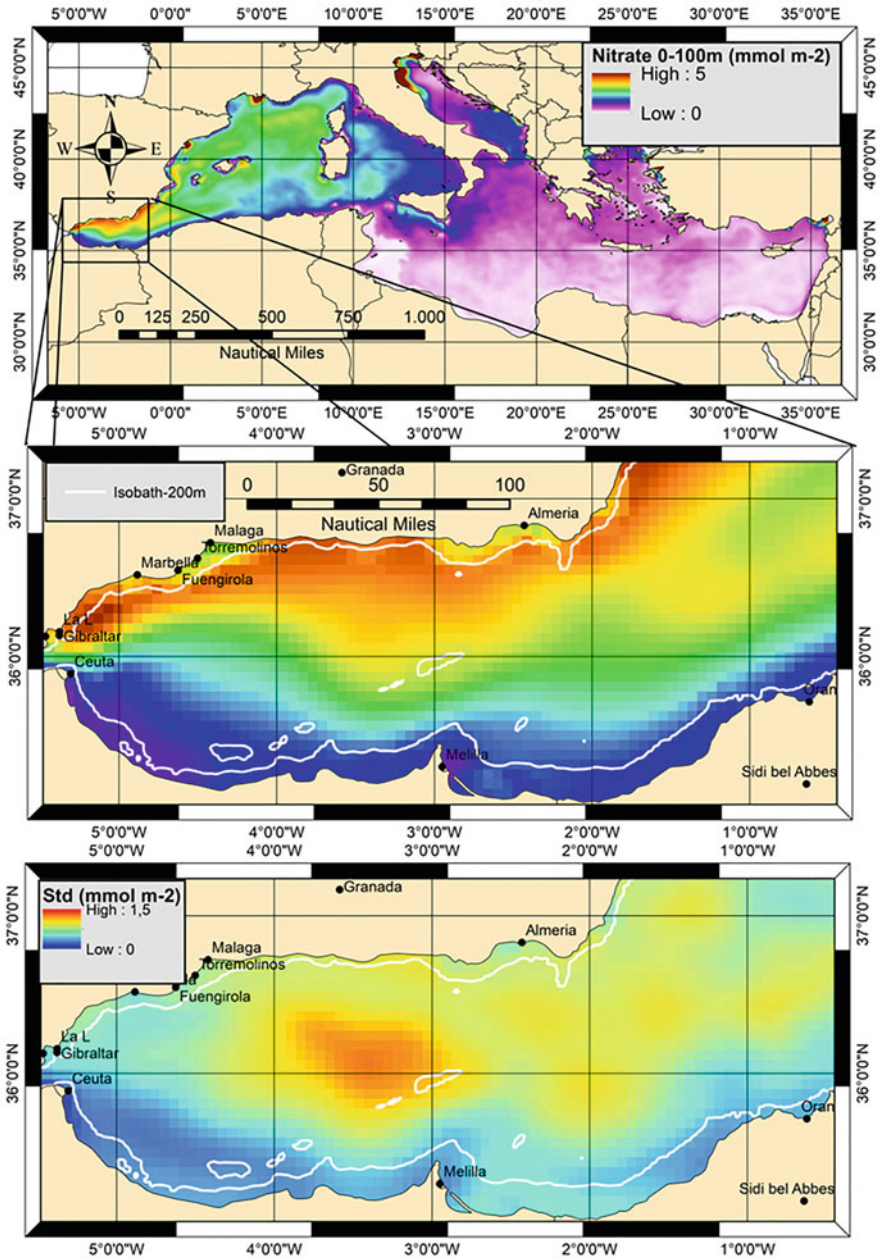


**Fig. 7.3** Mean spring (May) depth-integrated (0–100 m) nitrate concentration ( $\text{mmol}\cdot\text{m}^{-2}$ ) over the period 1999–2016: (a) in the Mediterranean basin, (b) in the Alboran Sea and (c) standard deviation. Generated using E.U. Copernicus Marine Service Information. (Product: MEDSEA\_REANALYSIS\_BIO\_006\_008) (Teruzzi et al. 2016) ([https://doi.org/10.25423/MEDSEA\\_REANALYSIS\\_BIO\\_006\\_008](https://doi.org/10.25423/MEDSEA_REANALYSIS_BIO_006_008))

(Morán and Estrada 2001). As the distance to the center of the gyres increases the nutricline uplifts rapidly, becoming shallower in the frontal areas associated to the WAG and the EAG (Arin et al. 2002; Reul et al. 2005; Leblanc et al. 2004; Mercado et al. 2014), due to the cross-frontal ageostrophic currents associated to the frontal systems in the western and eastern Alboran basin (Tintore et al. 1988, 1991). In both frontal areas the nutricline is usually found at <15 m depth (Morán and Estrada 2001; Reul et al. 2005; Leblanc et al. 2004).

In the continental margin of the NW Alboran Sea, the nutricline is roughly found at similar depths for nitrate, phosphate, and silicate (Ramírez et al. 2005; Ramírez 2007) and it is notably shallower than in open waters of the Alboran Sea. The banking of intermediate Mediterranean waters, circulating close to the border of the continental shelf (Parrilla and Kinder 1987), and the remineralization process in the water column could have a major role in the development of a shallower nutricline in this sector. On the other hand, the nutricline in this area of the Alboran Sea shows seasonal variations, being generally weak in winter, probably due to the mixing in the water column and to the influence of low nutrient water masses at intermediate depths (Ramírez 2007). The nutricline becomes steeper during the course of the year as the water column stratification develops (Ramírez et al. 2005; Ramírez 2007). In general, the nutricline in the continental margin is well developed in summer and also in early autumn, when the vertical profiles of nitrate, phosphate, and silicate are characterized by a relative maximum located around 50–75 m (Ramírez et al. 2005; Ramírez 2007), while this nutrient maxima is absent in winter and spring. At those maxima nutrient concentrations reach values close to  $\sim 7.0 \mu\text{M}$  for nitrate,  $\sim 0.35\text{--}0.40 \mu\text{M}$  for phosphate and  $\sim 4.0 \mu\text{M}$  for silicate, coinciding with a relative minimum of dissolved oxygen (Ramírez 2007). These findings suggest the occurrence of intense remineralization processes in the water column at shallower depths on the continental margin compared to remineralization processes in deeper areas of the westernmost sector of the Alboran Sea (Minas et al. 1991). At 200–300 m depth nutrients also show a high variability (Ramírez 2007). Thus, on the continental margin at 300 m depth the average nutrient concentrations are about  $\sim 8.5\text{--}10.0 \mu\text{M}$  for nitrate,  $\sim 0.4\text{--}0.5 \mu\text{M}$  for phosphate, and  $\sim 5.0\text{--}6.5 \mu\text{M}$  for silicate (Ramírez 2007). Further offshore nitrate concentrations are higher,  $\sim 12 \mu\text{M}$  at 300 m depth (García-Martínez et al. 2019).

On the other hand the vertical distribution of nitrite in the Alboran Sea shows a conspicuous subsurface maximum (Bianchi et al. 1994; Ramírez et al. 2005; Ramírez 2007; García-Martínez et al. 2019). In the Alboran Sea the presence of nitrite maximum is frequently observed throughout the all year (Ramírez 2007; García-Martínez et al. 2019). The highest values are usually found during the stratification period, with an average nitrite concentration close to  $0.3 \mu\text{M}$  (Ramírez et al. 2005; Ramírez 2007; García-Martínez et al. 2019). In the NW Alboran Sea this nitrite maximum is usually detected at depths ranging from 50 to 75 m (Fig. 7.2), frequently associated to the end of the nutricline (Ramírez et al. 2005; Ramírez 2007; García-Martínez et al. 2019). In the Almeria-Oran front area, the depth of the nitrite maximum have been found to range from  $\sim 40$  to 110 m (Bianchi et al. 1994), with the highest concentrations ( $>0.5 \mu\text{M}$ ) being found in the Atlantic waters adjacent to

the front, while in the rest of the areas nitrite maximum values were around  $0.2 \mu\text{M}$  (Bianchi et al. 1994). The nitrite maximum has been attributed to the oxidation of ammonium by nitrifying bacteria (Bianchi et al. 1994; Ramírez et al. 2005; Ramírez 2007), although the contribution from exudation by phytoplankton during the incomplete assimilatory reduction of nitrate cannot be disregarded (Ramírez 2007), since the nitrite maximum is frequently associated to the depth of the Chl-*a* maximum (Ramírez 2007; García-Martínez et al. 2019). However, it is noteworthy that the peak of nitrite is commonly found between the isohalines 37.0 and 37.5 (Ramírez et al. 2005; Ramírez 2007), which suggests that the Atlantic-Mediterranean interface could facilitate the accumulation of organic matter and the nitrification processes at this layer.

#### 7.2.4 Nutrient Molar Ratios: N or P Limitation?

It is accepted as a general paradigm that the molar ratio of dissolved inorganic N and P in the global ocean follows the ratio N:P (16:1), which reflects the general elemental composition of marine plankton (Redfield et al. 1963). In addition, Brzezinski (1985) found that the N:Si ratio for diatoms growing under optimal conditions was  $\sim 1:1$ . Based on these findings, it is widely assumed that the optimal N:Si:P ratios for marine phytoplankton is 16:16:1. Deviations from this elemental ratio have been extensively used to infer the potential limitation of phytoplankton growth by nutrients (Howarth 1988; Nelson and Dortch 1996). Departures of the theoretical Redfield ratio have been reported by many studies in different marine regions, including the Mediterranean Sea which is characterized by the extremely high N:P ratios (Krom et al. 1991; Ribera d'Alcalà et al. 2003). Thus, the N:P ratio in the intermediate water layer in the Eastern Mediterranean usually varies from 24 to 51, while in the deep Mediterranean waters it ranges from 25 to 30 (Ribera d'Alcalà et al. 2003). In addition, the intermediate and deep Mediterranean waters are also characterized by low N:Si ratios compared to the ratio 1:1. The N:Si ratio is generally lower than 1:1 in the Eastern Mediterranean, with values around  $\sim 0.90$  for intermediate waters and around  $\sim 0.5\text{--}0.6$  for deep waters (Ribera d'Alcalà et al. 2003). In the surface waters of the Eastern Mediterranean, where PP is strongly limited by P (Thingstad et al. 2005), the N:P and N:Si ratios are very variable ranging between  $<5\text{--}60$ , and  $1.7\text{--}18.2$ , respectively (Ribera d'Alcalà et al. 2003).

At difference from the Eastern Mediterranean, where P is the main limiting element for phytoplankton growth, the existing studies in the Alboran Sea and the Strait of Gibraltar suggest that N is the main limiting nutrient for phytoplankton growth in the surface layers (Dafner et al. 2003; Ramírez et al. 2005; Mercado et al. 2007, 2008; Ramírez 2007; Huertas et al. 2012). In the Gulf of Cadiz, the surface waters are characterized by N:P ratios  $<16:1$ , which suggests potential limitation of phytoplankton by N (Cravo et al. 2013). However, during its transits towards the Alboran Sea, the Atlantic waters coming from the Gulf of Cadiz are mixed and entrained with Mediterranean waters, while NACW cores are injected into the

Atlantic inflow. Due to these processes, as well as to phytoplankton consumption (Gómez et al. 2000), the elemental composition of Atlantic waters is modified along the Strait of Gibraltar. Several studies have reported that the N:P molar ratio in the Atlantic inflow is close to the Redfield ratio (Béthoux et al. 2002), while other studies found that the N:P molar ratio in the Atlantic water inflow tends to be lower than the Redfield ratio (16:1). Accordingly, Huertas et al. (2012) observed that the N:P ratios in the Atlantic waters at the Strait of Gibraltar ranged from 11 to 12, while the mean N:P ratio for the Mediterranean outflow was 17.5. The lower N:P ratios in the Atlantic layer were attributed to a preferential consumption of nitrate by phytoplankton in the Strait of Gibraltar and adjacent waters. Nevertheless, nitrate and phosphate in the Atlantic water inflow were higher than the half-saturation constant for both nutrients, hence these waters cannot be considered nutrient depleted (Huertas et al. 2012). Other studies found that the N:P ratios in the Atlantic water layer were higher at the Mediterranean side of the Strait of Gibraltar (on average 23.6) than on the Atlantic side (on average 13.8) (Dafner et al. 2003).

For the N:Si ratio the opposite pattern has been observed, i.e., higher average values on the western side of the Strait (1.46) and lower values on the eastern side (0.81) (Dafner et al. 2003). These eastward changes across the Strait of Gibraltar in the N:P and N:Si ratios within the Atlantic water layer are accompanied by changes in the phytoplankton community, with dinoflagellates dominating in the Atlantic side and diatoms at the eastern side (Gómez et al. 2000; Dafner et al. 2003). Dafner et al. (2003) estimated that physical and biological processes at the Strait could account for ~16% and ~84%, respectively, of the changes observed in the N:Si:P ratio at the Strait of Gibraltar. These authors suggested that the increase of the N:Si ratio at the eastern side of Strait could be due to uptake of Si by diatoms, similarly, the low phosphate concentrations ( $<0.02 \mu\text{M}$ ) at stations located at the eastern side of the Strait was also attributed an intense consumption of P by phytoplankton (Dafner et al. 2003). Nevertheless, the differences in the N:P values reported in the literature for the upper layers in the Strait of Gibraltar could also be due to the high spatio-temporal variability of hydrodynamic processes in this area (Gómez et al. 2000; Echevarría et al. 2002; Ramírez-Romero et al. 2014).

In the Alboran Sea, the nutrient molar ratios exhibit also high spatial and temporal variability in concordance with the high variability of nutrients. Figure 7.4 illustrates the spatial variability of the average integrated N:P ratio in the upper 100 m of the water column in the Mediterranean and the Alboran Sea in spring (May), reflecting a strong north-south gradient in the upper 100 m of the water column. However, as already mentioned different studies in the NW Alboran Sea have reported a deficiency of N relative to P in the surface layers when compared to the Redfield ratio (16:1) (Ramírez et al. 2005; Reul et al. 2005; Mercado et al. 2007). Thus, on the continental margin of NW Alboran Sea the average N:P ratio in the upper layer (0–20 m), i.e., at the depths where the Chl-a maximum is frequently found in this area (Ramírez et al. 2005; Ramírez 2007; García-Martínez et al. 2019), has been reported to range between ~2.0 and 14.0 (Ramírez et al. 2005; Ramírez 2007; Mercado et al. 2007). Reul et al. (2005) found N:P ratios lower than 16:1 above the nutricline and suggested a main role of N in regulating phytoplankton growth in



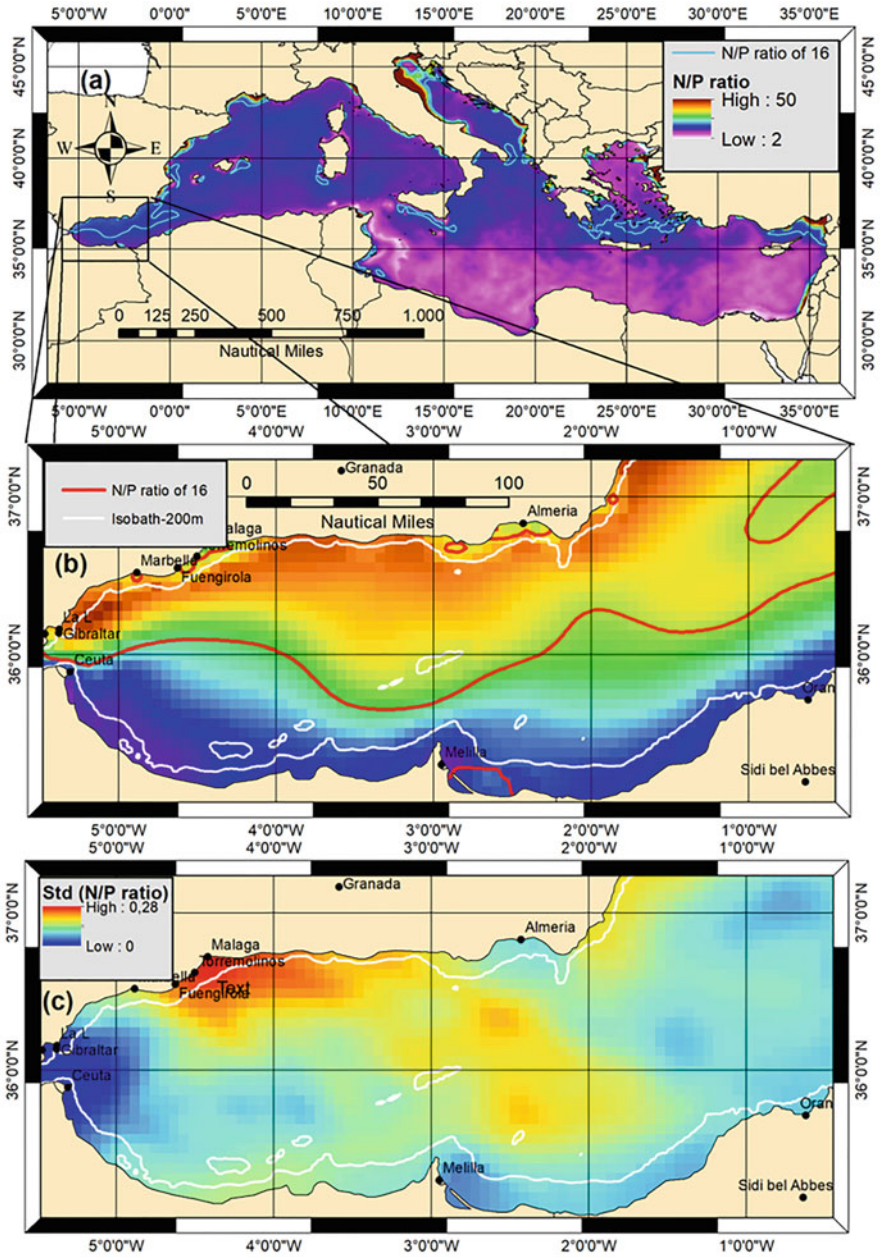


**Fig. 7.4** Mean spring (May) depth-integrated (0–100 m) N:P ratio over the period 1999–2016: (a) in the Mediterranean basin, (b) in the Alboran Sea, and (c) standard deviation. Generated using E.U. Copernicus Marine Service Information. (Product: MEDSEA\_REANALYSIS\_BIO\_006\_008) (Teruzzi et al. 2016) ([https://doi.org/10.25423/MEDSEA\\_REANALYSIS\\_BIO\\_006\\_008](https://doi.org/10.25423/MEDSEA_REANALYSIS_BIO_006_008))

the NW Alboran Sea, while below the nutricline N:P ratios were usually above 16:1. Higher N:P ratios (integrated values over 0–75 m) have been found by García-Martínez et al. (2019) along the northern continental margin of the Alboran Sea, where the average N:P ratio ranged between 13 and 16, depending on the time of the year, with an overall mean value of 15. On the other hand, the N:Si ratio shows values < 1:1 in the upper 20 m of the water column (Ramírez et al. 2005; Ramírez 2007). Thus, the average values for the N:Si ratio in the upper layers (0–20 m) in the NW sector of the Alboran Sea vary between <0.5 and ~0.8, which are lower than the ratio 1:1 for diatom growing under optimal conditions (Brzezinski 1985). The lowest N:P and N:Si ratios are found during summer-early autumn, coinciding with an intense stratification of the water column, while the higher ratios are usually observed in winter, when the water column is mixed, as well as in those periods of the year when the incidence of wind-driven upwelling is higher, usually during spring (Ramírez et al. 2005; Ramírez 2007; Mercado et al. 2007; Macías et al. 2007).

These low N:P and N:Si ratios in the upper 20 m, together with the relatively low nitrate concentrations during most time of the year, suggests that N plays a major role limiting the phytoplankton growth in the upper layers of this basin during great part of the year (Reul et al. 2005; Ramírez et al. 2005; Ramírez 2007). In addition, nitrate concentrations found in upper layers of the Alboran Sea are generally lower than the half-saturation constant ( $K_s$ ) ( $1 \mu\text{mol}\cdot\text{l}^{-1}$ ) for nitrate uptake by phytoplankton in coastal zones (MacIsaac and Dugdale 1969). All these findings support the hypothesis that in the Alboran Sea nitrate is the main limiting nutrient for phytoplankton. Thus, nitrate would control phytoplankton growth in winter and autumn when the Chl-a maximum is usually located at 0–20 m depth (Ramírez et al. 2005; García-Martínez et al. 2019), and also in summer and autumn at those shallow depths. However, during the stratification period, the Chl-a maximum becomes deeper, particularly in areas out of the influence of upwellings, being usually found at 50–75 m depth, i.e., below the seasonal thermocline and close to the limit of the photic layer, coinciding with lower limit of the nutricline (Ramírez 2007). At those depths nutrients should not be a limiting factor for phytoplankton, however, limitation by light may occur (Mercado et al. 2008). The hypothesis of the N-limitation in the NW Alboran Sea has been contrasted by additional experiments (Ramírez 2007) and is also supported by other facts. Thus, based on a 3 years study Ramírez (2007) found that on average the seasonal mean of the zonal wind component and nitrate concentration jointly explained ~80% of the temporal variability of the average seasonal Chl-a values, while the relationship with phosphate was weak. Likewise, Reul et al. (2005) found a correlation between cell (>2  $\mu\text{m}$ ) abundance and nitrate, while they did not find a relationship with phosphate. Recent studies (Lazzari et al. 2016) also found that, at difference from the rest of the Mediterranean, N is the main limiting nutrient in the Alboran Sea.

During upwelling events, the N:P ratio in recent upwelled waters reaches values >16:1 in the surface layers (0–20 m) while nitrate concentrations are usually >3  $\mu\text{M}$ , suggesting that there is no limitation by nitrate during the upwelling (Ramírez et al. 2005; Ramírez 2007). The intense upwellings in this area promote phytoplankton

bloom and a notable increase of Chl-a which can reach values  $>5 \mu\text{g}\cdot\text{l}^{-1}$  (Ramírez et al. 2005; Ramírez 2007). After cessation of westerlies a sharp decrease of nitrate has been reported, with concentrations dropping to undetectable levels at those stations with higher Chl-a concentration. This fast decline of nitrate is accompanied by a profound decrease of the N:P and N:Si ratios to values  $<2.0$  and  $<0.2$ , respectively (Ramírez et al. 2005; Ramírez 2007). This suggests that nitrate is rapidly and preferentially removed by phytoplankton during intense phytoplankton blooms, causing a rapid decline of both ratios. At the Strait of Gibraltar and the NW Alboran Sea, a preferential uptake of nitrate has also been reported by other studies (Reul et al. 2005; Huertas et al. 2012). The fast and preferential uptake of nitrate would explain the low nitrate concentrations usually found in the upper layers (0–20 m) in this sector of the Alboran Sea during large part of the year, except when upwelling events take place. The limitation by nitrate in the upper layers (0–20 m) is intermittently overcome by the upwelling events in the continental margin (Ramírez et al. 2005; Reul et al. 2005) which lead to an temporal enhancement of the N:P ratio and nitrate concentrations in the surface waters (0–20 m). Paradoxically, the fast and preferential uptake of nitrate during the blooms would shift the system towards N-limitation in a few days after the cessation of the upwelling event (Ramírez et al. 2005; Ramírez 2007).

The notable increase of the N:P and N:Si ratios in the upper layers (0–20 m) observed during wind-driven upwelling events has its origin in the strong vertical gradients of the N:P and N:Si molar ratios (Ramírez et al. 2005; Reul et al. 2005). In this area the N:P and N:Si ratios show a sharp increase with depth down to 50–100 m. The vertical gradients of both molar ratios are more marked during the stratification period. In contrast, vertical gradients are usually less marked in winter and also during intense upwelling events (Ramírez et al. 2005; Ramírez 2007). At 50 m depth, the average N:P molar ratios vary between  $\sim 13$  and 24, with most of the values above 15, while at 100 m depth the ratio increase to values ranging from  $\sim 19$  to 26 (Ramírez 2007). Therefore, in the NW Alboran Sea subsurface waters become strongly deficient in phosphate at depths  $\sim 100$  when compared to the Redfield ratio (16:1). At greater depths, the average N:P ratios continue increasing although more slowly, showing in general a weak maximum at 200 m where the average values ranged from  $\sim 20$  to  $\sim 27$ . At 300 m depth, the N:P ratio decreases slightly with average ratios varying between  $\sim 19$  and  $\sim 25$  (Ramírez 2007), with most of these values above 21. It is noticeable that the N:P ratios found at 200 m in the NW Alboran Sea are higher than the values found in deep waters of the Algero-Balear and Tyrrhenian basin (Ribera d'Alcalà et al. 2003). The high N:P values at shallower depths in the NW Alboran Sea can be attributed to respiration processes (Minas et al. 1991; Ramírez et al. 2005, 2006) and to the upwelling of intermediate Mediterranean waters on the continental slope during their transit towards the Strait of Gibraltar.

Similarly, the N:Si ratio also shows remarkable vertical gradients in the NW Alboran Sea, reaching on average maximum values at depths ranging from 50 m to 100 m throughout the year (Ramírez et al. 2005; Ramírez 2007), with a peak frequently observed in summer at 50 m. At that depth, the water column becomes deficient in silicate in relation to nitrate, with the average N:Si ratio varying between

~1 and ~2. Below 100 m depth, the ratio tends to decrease slowly with depth. In the NW Alboran Sea, at 300 m depth the average N:Si values ranged from ~1.5 to ~1.8 (Ramírez et al. 2005; Ramírez 2007). Crombet et al. (2011) found integrated (0–100 m) N:Si ratios >1 at the Strait of Gibraltar and at the eastern border of the Alboran Sea, which is consistent with the Si deficiency detected at shallow depths in the NW Alboran Sea. The higher N:Si ratios found at  $\geq 50$  m in the NW Alboran Sea could be due to a fast remineralization of nitrate in the water column compared to the dissolution of biogenic silica, even if the latter is accelerated by bacterial colonization (Bidle and Azam 2001).

In the Almeria-Oran frontal area, Leblanc et al. (2004) observed a strong P limitation in the photic layers. They found very low phosphate concentrations and high integrated N:P ratios in the photic layer at the frontal zone, the jet, and the adjacent waters. Thus, N:P ratios values of 24:1 were detected in the Atlantic waters adjacent to the front, while the highest N:P ratio (90:1) was associated to Mediterranean waters adjacent to the front. These findings are consistent with observations in the Algero-Balear basin, where P is in general the main limiting nutrient (Thingstad et al. 1998; Moutin and Raimbault 2002). The N:Si values in the photic layer of the Almeria-Oran front ranged from 0.32 to 0.83, while below the photic zone they obtained N:Si values ranging from 1.4 to 2.0 (Leblanc et al. 2004).

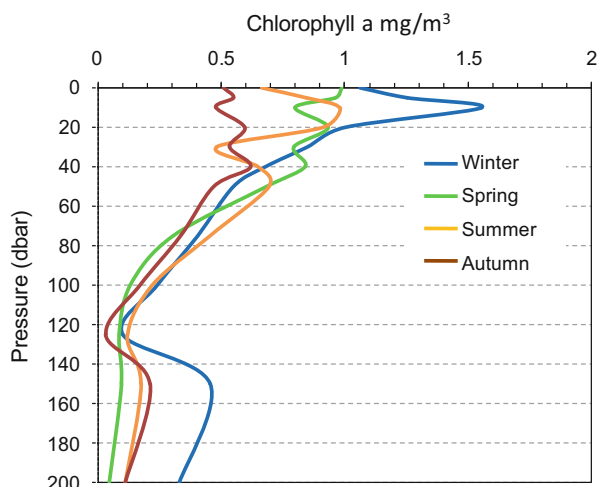
### **7.3 Phytoplankton Productivity: Coupling Between Physical, Biogeochemical, and Biological Features**

#### ***7.3.1 Distribution Patterns of Chlorophyll-a and Primary Production from In Situ Data***

The Alboran Sea is one of the most productive basins of the Mediterranean Sea. As previously discussed in this chapter, PP in the Alboran Sea is mainly related to wind-induced upwelling (particularly that forced by westerlies), mostly on the northern side of the WAG off the Spanish coast (Sarhan et al. 2000; Reul et al. 2005; Macías et al. 2007), and to the frontal ageostrophic circulation, associated to the path of the Atlantic jet, that induces upwelling at the periphery of the anticyclonic gyres (Sarhan et al. 2000; Garcia-Gorriz and Carr 1999, 2001). Therefore, any changes in the wind regime and the Atlantic jet characteristics may influence the dynamics and productivity of the Alboran Sea planktonic ecosystem (Garcia-Gorriz and Carr 2001; Ruiz et al. 2001; Macías et al. 2009; Oguz et al. 2014; Kersting 2016).

A number of studies have reported in situ data on Chl-a and/or PP distribution in the Alboran Sea (e.g., Morán and Estrada 2001; L'Helguen et al. 2002; Ramírez et al. 2005; Reul et al. 2005; Mercado et al. 2014; García-Martínez et al. 2019). Many of them have been conducted in the NW sector of the Alboran Sea, in particular in the area between Gibraltar and Marbella, as well as in the eastern side of the Strait of Gibraltar and the northern side of the WAG, since these are the most productive

**Fig. 7.5** Average seasonal vertical profiles (seasonal climatologies) of chlorophyll-a in the Alboran Sea (Manca et al. 2004). Source: Data and metadata are provided by the Italian National Oceanographic Data Center of the OGS Istituto Nazionale di Oceanografia e Geofisica Sperimentale (NODC/OGS), acting within the International Oceanographic Data Exchange System of the UNESCO Intergovernmental Oceanographic Commission (IOC) since 27/6/2002



areas in the Alboran Sea (as result of the different upwelling events previously described). The high productivity in these areas is reflected in high Chl-a concentrations and high phytoplankton abundance, in comparison with adjacent areas of the Western Alboran Sea, as those of the center of the WAG (Rodríguez et al. 1998; Reul et al. 2005; Mercado et al. 2014). In the Eastern Alboran Sea, when the EAG is well developed, the most productive zones are found at the northern edge of the EAG (Leblanc et al. 2004). But when the EAG collapses, Chl-a is enhanced at the southern part (Claustre et al. 1994).

As a general pattern, the upwelling area in the NW Alboran Sea is characterized by Chl-a concentrations higher than  $1 \mu\text{g}\cdot\text{l}^{-1}$  and high PP, whereas lower Chl-a concentrations ( $<1 \mu\text{g}\cdot\text{l}^{-1}$ ) and low PP are found in the central WAG (Rodríguez et al. 1998; Reul et al. 2005; Morán and Estrada 2001; Mercado et al. 2014). The southern sector of the Alboran Sea, occupied by nutrient-poor Atlantic waters, is characterized by low Chl-a concentrations and low PP. On the temporal scale, Chl-a concentration reaches maximum values in winter-spring (Fig. 7.5), when the surface waters present higher nutrients concentrations, while it decreases in summer-early autumn, when the water column is strongly stratified, (Ramírez et al. 2005; Mercado et al. 2007; García-Martínez et al. 2019). However, changes in the fertilization mechanisms previously described, together with changes in the light regime, lead to temporal changes of this pattern and the development of phytoplankton blooms (Prieto et al. 1999; Ramírez 2007; Mercado et al. 2007, 2008; Macías et al. 2008; García-Martínez et al. 2019). Furthermore, wind-driven upwelling along the Spanish coast provides episodic increases of Chl-a along the Spanish coast (Reul et al. 2005; Ramírez et al. 2005; García-Martínez et al. 2019). In the water column, a deep Chl-a maximum (DCM) is usually observed in the Alboran Sea during the stratified season, at depths between 50 m and 75 m (Fig. 7.5) (Rodríguez et al. 1998; Ramírez et al. 2005; Ramírez 2007; García-Martínez et al. 2019). Nevertheless,

the average profile of Chl-a in summer for the whole Alboran Sea presents also a shallower peak (Fig. 7.5), resembling the vertical profile in other areas of the Mediterranean (Lavigne et al. 2015). This shallower peak can be due to upwellings and advection of Chl-a patches. During the mixing period (late autumn to winter) the DCM is shallower or even disappear, with the higher Chl-a concentrations in the upper 20 m (Fig. 7.5) (Ramírez 2007; García-Martínez et al. 2019). In most of these cases, the Chl-a maximum is not properly a DCM, but a surface or subsurface maximum. In general, Chl-a concentration at the DCM in the Alboran Sea is commonly  $>0.5 \mu\text{g}\cdot\text{l}^{-1}$ , although values  $>1.0 \mu\text{g}\cdot\text{l}^{-1}$  are often found in the NW margin, where values close to  $\sim 8 \mu\text{g}\cdot\text{l}^{-1}$  can occasionally be found (Rodríguez et al. 1998; Ramírez et al. 2005; García-Martínez et al. 2019).

In the Alboran Sea PP decreases in general eastward, from the Strait of Gibraltar to Cape Gata. Although the existing in situ measurements of PP ( $^{14}\text{C}$ ) in the NW Alboran Sea reveal that there is also a decrease of the integrated PP (PPint) following a coast-offshore gradient, with the highest average values in the frontal area ( $632 \pm 184 \text{ mg}\cdot\text{C m}^{-2}\cdot\text{day}^{-1}$ ) and the lowest average values in the center of the WAG ( $330 \pm 149 \text{ mg}\cdot\text{C m}^{-2}\cdot\text{day}^{-1}$ ) (Morán and Estrada 2001). On the other hand, Macías et al. (2009) found that PPint varied between  $644 \text{ mg}\cdot\text{C m}^{-2}\cdot\text{day}^{-1}$  at the frontal area and  $6 \text{ mg}\cdot\text{C m}^{-2}\cdot\text{day}^{-1}$  at the western side of the Strait of Gibraltar (off Europa Point). In the Almería-Oran front (Eastern Alboran Sea), Semperé et al. (2003) estimated that the average PPint was around  $242 \text{ mg}\cdot\text{C m}^{-2}\cdot\text{day}^{-1}$  in the modified Atlantic jet area and the gyre, while it declined to  $117 \text{ mg}\cdot\text{C m}^{-2}\cdot\text{day}^{-1}$  in Mediterranean waters. Also in the Almería-Oran front and the Algerian Current the PP values at the frontal area ranged from 500 to  $1300 \text{ mg}\cdot\text{C m}^{-2}\cdot\text{day}^{-1}$  (with a mean value of  $880 \text{ mg}\cdot\text{C m}^{-2}\cdot\text{day}^{-1}$ ) (Lohrenz et al. 1988).

It has been hypothesized that in the absence of upwelling, the relatively low nitrate concentration found in the upper layers together with the low N:P and N:Si ratios, could favor the growth of a phytoplankton community of smaller cell size in NW Alboran Sea (Ramírez 2007), which are better adapted to grow in nutrient-deficient environments (Chisholm 1992) in comparison with other phytoplankton groups of larger cell size, such a diatoms. In fact several studies have reported that picoplankton and nanoplankton dominate the phytoplankton community in the surface layers of the Alboran Sea (Rodríguez et al. 1998; Arin et al. 2002; Reul et al. 2005). Moreover, temporal changes in the phytoplankton community at the continental margin of the NW Alboran Sea have been observed (Mercado et al. 2005, 2007). These changes, involving the shift of a phytoplankton community dominated by diatoms to a community dominated by coccolithophorids and small flagellates, were associated to changes in nitrate and the N:P the molar ratio. Moreover, taking into account that during great part of the year nitrate concentrations are low and that the N:P ratio is  $<16:1$ , it has been suggested that regenerated PP could be important in the NW Alboran Sea (Ramírez 2007). This is consistent with the low new PP values measured at the Almería-Oran front (mean value  $2.5 \text{ mmol}\cdot\text{m}^{-2}\cdot\text{day}^{-1}$ ) compared to other oceanic and coastal areas (L'Helguen et al. 2002). Low nitrate uptake rates (up to  $6.4 \text{ nmol}\cdot\text{l}^{-1}\cdot\text{h}^{-1}$ ) have been obtained in the frontal area, while maximum ammonium uptake rates were about

$13 \text{ nmol}\cdot\text{l}^{-1}\cdot\text{h}^{-1}$  (L'Helguen et al. 2002). The low new PP and nitrate uptake rates in the Almeria-Oran front could be caused by the low nitrate concentration in the photic layer and the relatively deep location of the nitracline (L'Helguen et al. 2002). In the NW Alboran Sea, the recurrence of intense upwelling events would temporarily overcome the limitation by nitrate, promoting phytoplankton blooms and a phytoplankton community dominated by diatoms (Gómez et al. 2000; Reul et al. 2005; Arin et al. 2002; Mercado et al. 2008, 2014). The rapid depletion of nitrate after the cessation of westerlies suggests that under the absence of upwelling, phytoplankton biomass and PP could be largely supported by regenerated forms of N. This is consistent with the findings of L'Helguen et al. (2002) who observed that PP in the Almeria-Oran front was initially nitrate-based, while regenerated production became gradually more important as nitrate was progressively consumed. In addition, average seasonal nitrate uptake rates in the upper layers of the NW Alboran Sea ranged from  $\sim 2$  to  $\sim 70 \text{ nmol N l}^{-1}\cdot\text{h}^{-1}$ , although most values were  $< 11 \text{ nmol N}\cdot\text{l}^{-1}\cdot\text{h}^{-1}$  (Mercado et al. 2008), which are close those reported by L'Helguen et al. (2002) in the Almeria-Oran front. In contrast, ammonium uptake rates ranged between  $\sim 5$  and  $86 \text{ nmol}\cdot\text{N l}^{-1}\cdot\text{h}^{-1}$  throughout the year (Mercado et al. 2008), with most of the mean seasonal values  $< 30.6 \text{ nmol N}\cdot\text{l}^{-1}\cdot\text{h}^{-1}$ . Higher uptake rates of both nitrate and ammonium were observed at the Chl-a maximum (Mercado et al. 2008).

However, most in situ measurements of Chl-a and PP have been carried out in particular areas of the Alboran Sea and did not cover either the whole Alboran basin or all the seasons. Over the last decades, several studies based on remote sensing data have analyzed the Chl-a and PP data in the whole Alboran Sea or in large parts of this basin, providing more comprehensive and synoptic information on the variability of phytoplankton biomass and PP in the Alboran Sea. This approach is discussed in the next section.

### ***7.3.2 Distribution Patterns of Chlorophyll-a and Primary Production from Satellite Derived Data Models***

#### **7.3.2.1 Sea Surface Chlorophyll-a Concentration from Satellite Data**

Surface Chl-a concentration as derived from satellite measurements allows detecting the main spatial and temporal patterns in the Mediterranean and the Alboran Sea (Morel and Andre 1991; Garcia-Gorriz and Carr 1999, 2001; Bosc et al. 2004; Macías et al. 2007). Based on Sea Surface Temperature (SST) and Chl-a concentration, Baldacci et al. (2001) defined two upwelling areas along the Spanish coast in the Alboran Sea: the first one is located between  $5.5^\circ \text{ W}$  and  $4.5^\circ \text{ W}$ , and the second one is located between  $4.5^\circ \text{ W}$  and  $2^\circ \text{ W}$ . The first area (A) is associated to the NW Alboran upwelling area and it stretches from the Strait of Gibraltar to Cape Pino (Malaga). The second upwelling area (B) extends from Cape Pino to Cape Gata (Almeria), the named Atlantic-Mediterranean Transition zone (Muñoz et al. 2017).

Both areas are characterized by the presence of waters upwelled by westerlies and/or cyclonic circulation cells (Baldacci et al. 2001), but they differ in their upwelling patterns throughout the year. Although the upwelling occurs simultaneously in both areas in spring and early autumn (October), higher Chl-a concentrations are found in area B in late autumn. In contrast in winter (January to March) and in summer higher Chl-a are found in area A.

In addition, the upwelling associated to the frontal area of the Atlantic jet is also a distinctive feature from Chl-a satellite data. The periphery of the WAG becomes richer in Chl-a as the jet travels through the Alboran Sea, due to the in situ growth of phytoplankton and also due to advection of Chl-a patches from nearby areas (Ruiz et al. 2001; Garcia-Gorriz and Carr 2001; Arin et al. 2002; Macías et al. 2007). On the other hand, according to Garcia-Gorriz and Carr (2001) the Chl-a annual cycle in the Alboran is in general characterized by a bloom period (November to March) and a non-bloom period (May to September), with transition periods between these two regimes. Other studies in the NW Alboran Sea based on satellite data have reported an intense bloom in March–April (Macías et al. 2007), declining the Chl-a values from June to September and increasing again from September to December. Lazzari et al. (2012), based on a 6 years study of satellite data for the whole Alboran basin, found the lower Chl-a values from June to September and higher values from November to May. Nevertheless, the interannual variability of Chl-a in the Alboran Sea is very high (Bosc et al. 2004) and its seasonal cycle, as derived from satellite data, is the most chaotic of the Mediterranean Sea (Bosc et al. 2004), with a minimum in summer ( $\sim 0.20\text{--}0.25 \mu\text{g Chl-a}\cdot\text{l}^{-1}$ ).

While satellite images are limited to surface waters, 3D models allow integration of Chl-a and other variables in the water column (Lazzari et al. 2012). Figure 7.6 shows comparatively the mean integrated Chl-a values (1999–2016) during the month of May, one of the most productive months in the Alboran Sea according to the results of Lazzari et al. (2012), for the whole Mediterranean Sea and the Alboran Sea. Figure 7.6b shows a marked eastward gradient of Chl-a in the Alboran Sea with large differences between the western and the eastern basin. According to this Figure, in the western basin very high Chl-a concentrations are observed in spring in the NW sector off Malaga Bay, while very low values are found at the Strait of Gibraltar and in the westernmost part of the Alboran Sea. These low Chl-a values could be due to a time lag in the response of phytoplankton to the injection of nutrient into the euphotic layer. Some authors have argued that due to the high velocity of the Atlantic jet in the vicinities of the Strait, nutrients would have a quasi-conservative behavior (Minas et al. 1991). Thus the combined effect of the speed of the Atlantic jet and the time lapse for building phytoplankton biomass may result in low integrated Chl-a values at the vicinities of the Strait. Figure 7.6b also shows high Chl-a concentrations covering the entire eastern Alboran basin, probably due to the effect of wind-driven upwelling at this time of the year and the advection towards the center of the basin, although the values are slightly lower than those observed off the Malaga Bay. The higher variability is found between Marbella and Malaga due to intermittent upwelling processes (Fig. 7.6c).



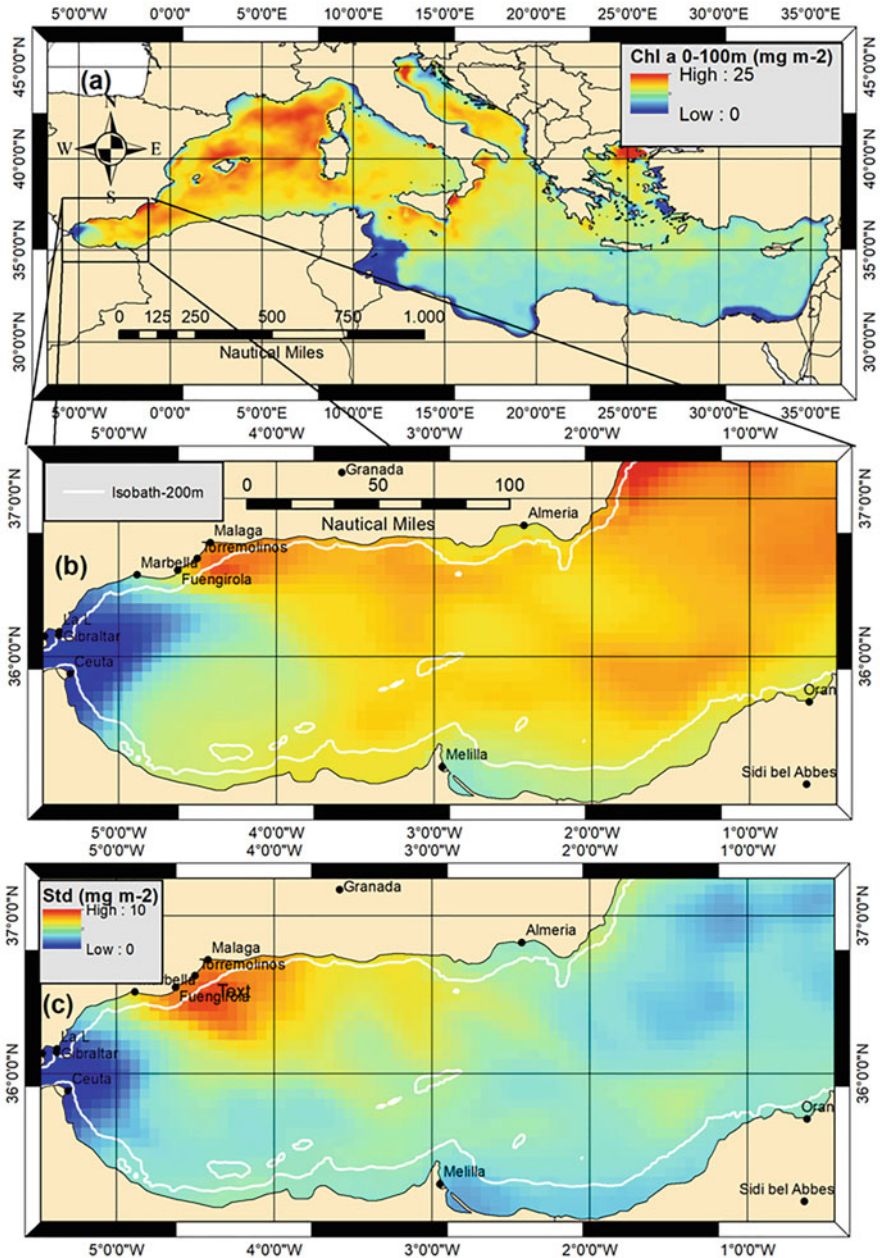


**Fig. 7.6** Mean spring (May) depth-integrated (0–100 m) chlorophyll-a (mg·m<sup>-2</sup>) over the period 1999–2016: (a) in the Mediterranean basin, (b) in the Alboran Sea and (c) standard deviation. Generated using E.U. Copernicus Marine Service Information. (Product: MEDSEA\_REANALYSIS\_BIO\_006\_008) (Teruzzi et al. 2016) ([https://doi.org/10.25423/MEDSEA\\_REANALYSIS\\_BIO\\_006\\_008](https://doi.org/10.25423/MEDSEA_REANALYSIS_BIO_006_008))

### 7.3.2.2 Primary Production from Satellite Data

According to Spalding et al. (2007), the Alboran Sea is an ecoregion included in the Mediterranean province, defined in general as a low productivity ecosystem ( $<150 \text{ g C}\cdot\text{m}^{-2}\cdot\text{year}^{-1}$ ) (Aquarone et al. 2009). However, at smaller regional scales within the Mediterranean, there is high spatial and temporal variability in PP. Thus, Bosc et al. (2004), analyzed 4 year mean PP values derived from satellite images for different Mediterranean Sea regions, and concluded that the Alboran Sea is the most productive region of the Mediterranean, with an average annual PP of  $230 \text{ g C}\cdot\text{m}^{-2}\cdot\text{year}^{-1}$ , being this value almost  $100 \text{ g C}\cdot\text{m}^{-2}\cdot\text{year}^{-1}$  higher than the overall mean for the Mediterranean basin. These values are in agreement with the results obtained by Antoine et al. (1995), who estimated a mean PP of  $156 \text{ g C}\cdot\text{m}^{-2}\cdot\text{year}^{-1}$  for the Mediterranean and  $250 \text{ g C}\cdot\text{m}^{-2}\cdot\text{year}^{-1}$  for the Alboran Sea. Based on a 3D-biogeochemical model (1999–2004) Lazzari et al. (2012), estimated for the Alboran Sea a net PP (NPP) of  $274 \pm 11 \text{ g C}\cdot\text{m}^{-2}\cdot\text{year}^{-1}$  and classified this basin as mesotrophic (integrated NPP between 100 and  $300 \text{ g C}\cdot\text{m}^{-2}\cdot\text{year}^{-1}$ ), showing the NPP a clear seasonal pattern with higher values between January and June and the highest peaks between February and May (Lazzari et al. 2012).

Figure 7.7 shows the spatial heterogeneity of PP in the upper 100 m in the Mediterranean and the Alboran Sea in spring (May), which according to the results of Lazzari et al. (2012) is one of the most productive months in the Alboran Sea. The depth-integrated (0–100 m) PP of the whole Mediterranean Sea depicts the Alboran Sea as the most productive region (Fig. 7.7a). In spite of being the region with the highest integrated NPP of the Mediterranean Sea, it is noteworthy to mention the existence of very strong spatial differences within the Alboran Sea, with zones where PP values are extremely low and others with extremely high values (Fig. 7.7b). The areas with the highest PP ( $0.6 \text{ g C}\cdot\text{m}^{-2}\cdot\text{day}^{-1}$ ) are located in the northern part of the Alboran Sea (between Malaga and Motril) and the southern part of the eastern basin (off the eastern Moroccan coasts) (Fig. 7.7b). These values extrapolated to the whole year would result in a mean PP of  $219 \text{ g C}\cdot\text{m}^{-2}\cdot\text{year}^{-1}$ , which is similar to the value given by Lazzari et al. (2012). On overall, Fig. 7.7b illustrates the coexistence in the Alboran Sea of oligotrophic, poor Chl-a, and low productive areas, together with mesotrophic, rich Chl-a, and high productive areas.

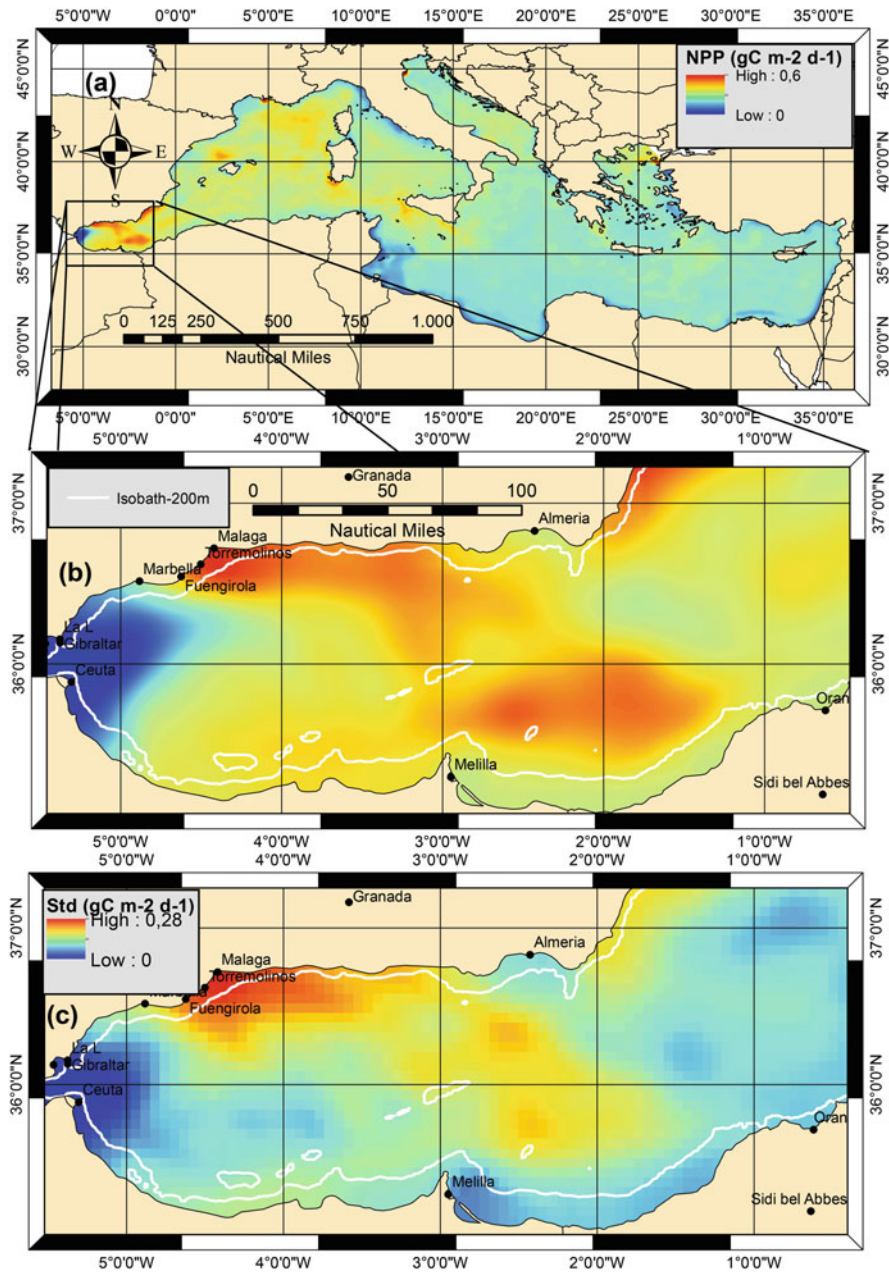


**Fig. 7.7** Mean spring (May) depth-integrated (0–100 m) net primary production ( $\text{g C}\cdot\text{m}^{-2}\cdot\text{day}^{-1}$ ) over the period 1999–2016: (a) in the Mediterranean basin, (b) in the Alboran Sea and (c) standard deviation. Generated using E.U. Copernicus Marine Service Information. (Product: MEDSEA\_REANALYSIS\_BIO\_006\_008) (Teruzzi et al. 2016) ([https://doi.org/10.25423/MEDSEA\\_REANALYSIS\\_BIO\\_006\\_008](https://doi.org/10.25423/MEDSEA_REANALYSIS_BIO_006_008))

## 7.4 Future Scenarios in the Framework of a Changing Climate

### 7.4.1 *Analyzing the Possible Effects of Climate Change on Water Circulation, Nutrients, and Primary Productivity in the Mediterranean and the Alboran Sea*

Climate change is expected not only to affect oceanic conditions worldwide (IPCC 2007, 2013; Reid et al. 2009) but also to induce changes in water mass properties and their associated circulation patterns. As result of changes in water temperature, stratification, vertical mixing, or in nutrient or light availability, water biochemistry, and marine ecosystems may be modified (Bopp et al. 2001; Boyd and Doney 2002; Sarmiento et al. 2004; Steinacher et al. 2010; Taucher and Oschlies 2011).

Due to its modest dimensions, Mediterranean Sea is very sensitive and may respond rapidly to environmental changes (atmospheric forcing and anthropogenic influences) (Béthoux and Gentili 1999; Lejeusne et al. 2010; Lionello et al. 2010; Schroeder et al. 2012, 2017). Expected future changes in the Mediterranean Sea include an increase in seawater temperature and salinity, reductions in freshwater inputs (precipitation and river inflow), changes in the ocean-atmosphere heat flux, and an increase in human pressure (Béthoux and Gentili 1999; Vargas-Yáñez et al. 2008; Sanchez-Gomez et al. 2011; Borghini et al. 2014; García-Martínez et al. 2017; Macías et al. 2018). All these factors play a crucial role in dense water formation and hence they determine the circulation in the Mediterranean Sea (Mediterranean Thermohaline Circulation—MTHC) (Béthoux and Gentili 1999). Changes in circulation can reduce the supply of nutrients, therefore geochemical cycles and PP (also affected through changes in temperature, pH, light availability, or in atmospheric and terrestrial inputs of nutrients) of the Mediterranean Sea will be altered (Sarmiento et al. 2004; Durrieu de Madron et al. 2011; IPCC 2013; Lazzari et al. 2014; Macías et al. 2014b).

Some studies have carried out a set of numerical experiments to quantify the sensitivity of the Mediterranean Sea to the twenty-first century climate change (Adloff et al. 2015). The projections of the possible effects of climate change on water circulation, nutrients, and primary productivity are studied by developing “scenarios” (the IPCC SRES, Nakicenovic and Swart 2000). A scenario is a description of a hypothetical future development of the Earth’s societies and economies. The Intergovernmental Panel on Climate Change “Special Report on Emissions Scenarios” (SRES) explored pathways of future greenhouse gas emissions, derived from self-consistent sets of assumptions about energy use, population growth, economic development, and other factors. Considering the temperature rise by 2100, the “hottest” scenario is A1FI, followed by A2, A1B, B2, A1T; and B1 is the “coolest.” However, in the A1B and A1T fossil CO<sub>2</sub> emissions are falling by 2100, whereas in A2 and B2 they are still rising, implying that climate impacts would be greater during the following century. In scenarios A1FI, B1, and B2, CO<sub>2</sub> emissions from land-use change drop below zero.

These scenarios are used to force models of different complexity and resolution (Lazzari et al. 2014). There are different types of models: General circulation models (GCM), higher resolution regional ocean models, or coupled atmosphere-ocean regional climate models (RCSM), but global models with low spatial resolution cannot sufficiently resolve the local and mesoscale processes that characterize the Mediterranean region (Jordá et al. 2011; Gomis et al. 2016; Akhtar et al. 2018), even less the Alboran Sea. The use of RCSM for future projections started recently with Somot et al. (2008) and Carillo et al. (2012) studies, followed by the European project CIRCE (Dubois et al. 2012; Gualdi et al. 2013) and actually in the Med-CORDEX initiative (Ruti et al. 2016). In this section, we present a detailed summary of different studies that have analyzed the projections obtained from models on the evolution of physical, chemical, and biological properties during the twenty-first century in the Mediterranean Sea.

The first attempt to predict the effect of ocean warming on the Mediterranean Sea circulation was the one by Thorpe and Bigg (2000). These authors used ocean and air-sea fluxes models with the low resolution which predicted a weakening of the MTHC in a scenario of  $2\times\text{CO}_2$ . In the same way, Somot et al. (2006) using A2 scenario (IPCC SRES) obtained projections with higher resolution models that show an increase of sea surface temperature (SST) and salinity (SSS), and also a strong weakening of the MTHC and changes in the characteristics of the Mediterranean outflow. Somot et al. (2008) improved simulations by developing a global atmospheric model coupled with a high-resolution oceanic model of the Mediterranean Sea. Simulations for the period 1960–2099 performed in a SRES-A2 scenario showed once again an increase of the surface temperature in the Mediterranean basin.

Under the umbrella of the EU project SESAME (Lazzari et al. 2014), ecosystem models were developed to connect low and high trophic levels and basin scale models to execute scenario simulations (the IPCC SRES, A1B scenario) for the future (2070–2100). The results obtained for the twenty-first century simulations showed: (1) an upper layer warming that enhances photosynthesis and increase Gross Primary Productivity (higher in the Eastern Mediterranean Sea) and (2) an increase in the vertical stability of the water column which limits the nutrient vertical supply into the euphotic zone and therefore improves the microbial loop of the marine trophic web. The maximum increase of temperature is achieved in the Alboran Sea during wintertime and the primary productivity maps show a strong positive signal in the Alboran Sea.

The projections of models developed under the framework of the EU project CIRCE (Gualdi et al. 2013) show a decrease of the surface net heat loss during the twenty-first century. Dubois et al. (2012) study presented projections under A1B scenario for the period 1950–2050 and found a decrease in the heat loss and an increase in water loss, which may affect the Mediterranean water masses and the associated MTHC. Numerous studies have been carried out within the framework of the Med-CORDEX initiative, such as the study conducted by Harzallah et al. (2018), which evaluates the Mediterranean Sea heat budget components. Results for the period 1990–2010 show positive and significant trends in the temperature of the

outflowing water through the Strait of Gibraltar. In addition, other projects such as VANIMEDAT-2 (Jordá et al. 2011) aimed at exploring the sea level variability under climate change scenarios for the twenty-first century.

NEMOMED oceanic models are regional versions of the NEMO model on the Mediterranean basin with different spatial resolutions: NEMOMED-12 (Waldman et al. 2017), NEMOMED-16 (Soto-Navarro et al. 2015) or NEMOMED-8. NEMOMED-8 model (Beuquier et al. 2010) has a horizontal resolution from 9 to 12 km (North to South). The circulation through the strait is simulated with realistic Atlantic Waters (AW). These models are used for coupled system regional climate system models (RCSMs) (Sevault et al. 2014; Adloff et al. 2015), which include a high-resolution and fully coupled representation of most of the physical components of the regional climate system (atmosphere, land surface, vegetation, hydrology, rivers, and ocean). Padorno et al. (2012) observed in their simulations for 140 years (1960–2099) with NEMOMED-8 that the main changes are warming and saltening waters, mean sea level increase, thermohaline circulation variations, and that deep water convection changes. Adloff et al. (2015) study the period 2001–2099 (NEMOMED-8), following different socio-economic scenarios (IPCC SRES). In most of the cases, they found an increase in the future Mediterranean SST and SSS and that MTHC tends to reach a situation similar to the Eastern Mediterranean Transient (EMT). The EMT, which took place in the Aegean Sea from 1988 to 1995, is considered the most relevant intermediate to deep Mediterranean overturning perturbation registered by instrumental records (Tsimplis et al. 2006; Roether et al. 2007, 2014; Lejeune et al. 2010; Incarbona et al. 2016). In the 1990s, the Aegean Sea began to discharge unusually dense waters inducing the so-called EMT which was caused by the accumulation of high salinity waters in the Levantine and enhanced heat loss in the Aegean Sea, coupled with surface water freshening in the Sicily Channel.

Richon et al. (2018) used NEMOMED-8 coupled with biogeochemical model PISCES. In an A2 IPCC SRES scenario, projections for the twenty-first century indicate a warming, increased stratification, and changes in Atlantic and river inputs which can lead to an accumulation of nitrate (whereas no for phosphorus) in the Mediterranean Sea and a decrease in biological productivity. Most coupled climate–marine biogeochemical models also predict a decline in NPP in the coming decades as a response to global warming (Bopp et al. 2001, 2013; Steinacher et al. 2010).

Multi-model projections, such as the ones obtained from the World Climate Research Program Coupled Model Intercomparison Project Phase 3 (CMIP3) multi-model projections have been used to analyzed hydroclimatic changes in the Mediterranean over the twenty-first century (Mariotti et al. 2008). By 2070–2099, the CMIP3 multi-model projections predict an increase in the loss of freshwater over the Mediterranean Sea due to precipitation reduction and warming-enhanced evaporation. The decrease in river runoff from the surrounding land will further exacerbate the increase in the Mediterranean Sea freshwater deficit.

There are very few modeling studies about the effects of climate change on plankton community and productivity in the Mediterranean Sea. The MERMEX program aims to study the response of Mediterranean ecosystems to natural and

anthropogenic pressures and combines integrated observation/experimentation/modeling approaches. Durrieu de Madron et al. (2011) reviewed the state of the current functioning and responses of Mediterranean marine biogeochemical cycles and ecosystems and concluded the need for international multi-disciplinary research coupling experiments, long-term observations, eco-regionalization, and modeling.

Herrmann et al. (2014) study represents one of the first attempts to model and assess the effects of the oceanic and atmospheric long-term evolution of the pelagic planktonic ecosystem, using a 3D coupled physical-biogeochemical model focusing only on the NW Mediterranean Sea. In Macías et al. (2018) a coupled model system is also used to explore potential changes in future scenarios (~2030) in the deep convection, in the euphotic layer fertilization, and the impact on phytoplankton and primary productivity in the NW Mediterranean Sea. Their results show an increase in the strength and duration of the annual deep convection event (which is the main trigger of the typical phytoplankton bloom of this area) and changes in the seasonal plankton cycles. On the other hand, Macías et al. (2015) present the results of a 3D hydrodynamic-biogeochemical coupled model (for the entire Mediterranean Sea). Simulations under two emission scenarios showed that the western basin becomes more oligotrophic due to a surface density decrease (increase stratification) because of the influence of the Atlantic waters that prevents surface salinity to increase.

Another important stressor is acidification and one of the EU initiatives that have addressed this issue in the Mediterranean is the MedSea project, which aimed at forecasting changes in the Mediterranean Sea driven by increases in CO<sub>2</sub> and other greenhouse gases, while focusing on the combined impacts of acidification and warming on the marine shell and skeletal building, productivity, and food webs. The combined effect of Mediterranean seawater acidification with warming on Mediterranean biogeochemistry, and ecosystems, through direct impacts on its highly adapted calcareous and non-calcareous organisms, may be larger than in other regions (<http://medsea-project.eu/>). The Mediterranean Sea is acidifying quickly (Goyet et al. 2016). Up to 30% of the anthropogenic CO<sub>2</sub> remains in the upper 200 m of the water column (Sabine et al. 2004). The acidification of the euphotic layer (Sabine et al. 2004; Orr et al. 2005) can affect physiological processes and the composition of the phytoplankton community (Reul et al. 2014). Current signals point to the reduction in the rate of calcification in phytoplankton (mainly coccolithophores), which could lead to changes both in marine ecosystems and in the carbon cycle. Nevertheless, there is no a consensus and different studies conjecture the widely varying responses under elevated pCO<sub>2</sub> (Beaufort et al. 2011; Álvarez et al. 2014; Meier et al. 2014; Dutkiewicz et al. 2015).

In general, climate projections tend to agree, with relatively high confidence, that the Mediterranean region will experience higher temperatures and reduced rainfall in the coming decades (IPCC 2013). In consequence, as climate model projections show, there will be increasing rates of evaporation and salinification of the Mediterranean Sea over the twenty-first century under anthropogenic greenhouse gas emission scenarios (Giorgi and Lionello 2008; Somot et al. 2008; Mariotti et al. 2008, 2015; Adloff et al. 2015). Mediterranean thermohaline circulation may significantly change by weakening in the western basin and a less certain response in

the eastern basin (Somot et al. 2006; Adloff et al. 2015). Changes in thermohaline circulation can profoundly affect the biogeochemistry of the Mediterranean Sea (Powley et al. 2018) and through an increase of stratification (Herrmann et al. 2014; Adloff et al. 2015) may reduce the nutrient supply into the euphotic layer with consequences for phytoplankton blooms (D'Ortenzio and Ribera d'Alcalà 2009; Herrmann et al. 2013).

Potential effects of the climatic scenario have also been described for the Alboran Sea circulation (Macías et al. 2018), and for the upwelling in the NW of Alboran Sea, strongly influenced by the Atlantic water entering through the Strait of Gibraltar and that could be affected by a generalized slowdown of the thermohaline circulation (Macías et al. 2014a).

Mediterranean Sea phosphate and nitrate concentrations seem to be more dependent on atmospheric and terrestrial inputs than on the Atlantic influx across the Strait of Gibraltar (Béthoux et al. 1998; Ribera d'Alcalà et al. 2003; Durrieu de Madron et al. 2011). Since the beginning of the industrial era, there has been an overall increase in atmospheric deposition (Duce et al. 2008) that might be higher in the coming years. These changes coupled with the expected decrease in winter mixed layer depth, could result in changes in the relative availability of nutrients, and increase the relative importance of atmospheric inputs in the Mediterranean Sea. Expected consequences are an imbalance between nitrate and phosphate concentrations in surface waters, causing changes in the phytoplankton populations and in the entire food web (Pasqueron 2015).

**Acknowledgments** This study has been conducted using E.U. Copernicus Marine Service Information. We are grateful to OGS (Istituto Nazionale di Oceanografia e Geofisica Sperimentale) for providing the data of the average vertical profiles (annual climatologies) of nutrients and dissolved oxygen, and the average seasonal vertical profiles (seasonal climatologies) of chlorophyll-a for the Alboran Sea (Manca et al. 2004) (Source: Data and metadata are provided by the Italian National Oceanographic Data Center of the OGS Istituto Nazionale di Oceanografia e Geofisica Sperimentale (NODC/OGS), acting within the International Oceanographic Data Exchange System of the UNESCO Intergovernmental Oceanographic Commission (IOC) since 27/6/2002). We thank Dr. Juan Pérez de Rubín (Instituto Español de Oceanografía, IEO) for providing the nutrient data collected during the IctioAlboran0793 survey.

## References

- Adloff F, Somot S, Sevault F et al (2015) Mediterranean Sea response to climate change in an ensemble of twenty first century scenarios. *Clim Dyn* 45(9–10):2775–2802
- Akhtar N, Brauch J, Ahrens B (2018) Climate modeling over the Mediterranean Sea: impact of resolution and ocean coupling. *Clim Dyn* 51(3):933–948
- Álvarez M, Sanleón-Bartolomé H, Tanhua T et al (2014) The CO<sub>2</sub> system in the Mediterranean Sea: a basin wide perspective. *Ocean Sci* 10:69–92
- Antoine D, Morel A, André J-M (1995) Algal pigment distribution and primary production in the eastern Mediterranean as derived from coastal zone color scanner observations. *J Geophys Res* 100(C8):16193–16209



- Aquarone MC, Adams S, Mifsud P (2009) LMEs and regional seas IV Mediterranean Sea. 187–200. <https://iwlearn.net/resolveuid/8616e8d55e78e743f073896667472210>. Accessed 22 Jan 2019
- Arin L, Morán XAG, Estrada M (2002) Phytoplankton size distribution and growth rates in the Alboran Sea (SW Mediterranean): short term variability related to mesoscale hydrodynamics. *J Plankton Res* 24(10):1019–1033
- Bakun A, Agostini VN (2001) Seasonal patterns of wind-induced upwelling/downwelling in the Mediterranean Sea. *Sci Mar* 65(3):243–257
- Balbín R, López-Jurado LJ, Aparicio-González A et al (2014) Seasonal and interannual variability of dissolved oxygen around the Balearic Islands from hydrographic data. *J Mar Syst* 138:51–62
- Baldacci A, Corsini G, Grasso R et al (2001) A study of the Alboran Sea mesoscale system by means of empirical orthogonal function decomposition of satellite data. *J Mar Syst* 29(1–4):293–311
- Beaufort L, Probert I, de Garidel-Thoron T et al (2011) Sensitivity of coccolithophores to carbonate chemistry and ocean acidification. *Nature* 476:80–83
- Béthoux JP, Gentili B (1999) Functioning of the Mediterranean Sea: past and present changes related to freshwater input and climate changes. *J Mar Syst* 20(1–4):33–47
- Béthoux JP, Morin P, Madec C et al (1992) Phosphorus and nitrogen behaviour in the Mediterranean Sea. *Deep-Sea Res* 39(9):1641–1654
- Béthoux JP, Morin P, Chaumery C et al (1998) Nutrients in the Mediterranean Sea, mass balance and statistical analysis of concentrations with respect to environmental change. *Mar Chem* 63(1–2):155–169
- Béthoux JP, Morin P, Ruiz-Pino DP (2002) Temporal trends in nutrient ratios: chemical evidence of Mediterranean ecosystem changes driven by human activity. *Deep Sea Res II* 49:2007–2016
- Beuvier J, Sevault F, Herrmann M et al (2010) Modeling the Mediterranean Sea interannual variability during 1961–2000: focus on the Eastern Mediterranean transient. *J Geophys Res Oceans* 115:C08017. <https://doi.org/10.1029/2009JC005950>
- Bianchi M, Morin P, Le Corre P (1994) Nitrification rates, nitrite and nitrate distribution in the Almeria-Oran frontal system (eastern Alboran Sea). *J Mar Syst* 5(3–5):327–342
- Bidle KD, Azam F (2001) Bacterial control of silicon regeneration from diatom detritus: Significance of bacterial ectohydrolases and species identity. *Limnol Oceanogr* 46(7):1606–1623
- Bopp L, Monfray P, Aumont O et al (2001) Potential impact of climate change on marine export production. *Global Biogeochem Cy* 15(1):81–99
- Bopp L, Resplandy L, Orr JC et al (2013) Multiple stressors of ocean ecosystems in the 21st century: projections with CMIP5 models. *Biogeosciences* 10:6225–6245
- Borghini M, Bryden H, Schroeder K et al (2014) The Mediterranean is becoming saltier. *Ocean Sci* 10:693–700
- Bosc E, Bricaud A, Antoine D (2004) Seasonal and interannual variability in algal biomass and primary production in the Mediterranean Sea as derived from 4 years of SeaWiFS observations. *Global Biogeochem Cy* 18:GB1005. <https://doi.org/10.1029/2003GB002034>
- Boyd PW, Doney SC (2002) Modelling regional responses by marine pelagic ecosystems to global climate change. *Geophys Res Lett* 29(16):1086. <https://doi.org/10.1029/2001GL014130>
- Bruno M, Alonso JJ, Cózar A et al (2002) The boiling water phenomena at Camarinal Sill, the Strait of Gibraltar. *Deep-Sea Res II* 49(19):4097–4113
- Brzezinski MA (1985) The Si:C:N ratio of marine diatoms: interspecific variability and the effect of some environmental variables. *J Phycol* 21(3):347–357
- Cano N, García Lafuente J (1991) Corrientes en el litoral malagueño. Baja frecuencia. *Bol Inst Esp Oceanogr* 7(2):59–77
- Cano N, García Lafuente J, Hernández-Guerra A et al (1997) Hidrología del mar de Alborán en julio de 1993. *Publ Espec Inst Esp Oceanogr* 24:9–26
- Carillo A, Sannino G, Artale V et al (2012) Steric sea level rise over the Mediterranean Sea: present climate and scenario simulations. *Deep-Sea Res II* 39(9–10):2167–2184

- Chisholm SW (1992) Phytoplankton size. In: Falkowski PG, Woodhead AD (eds) Primary productivity and biogeochemical cycles in the sea. Woodhead, Plenum Press, New York, pp 213–237
- Claustre H, Kerhervé P, Marty JC et al (1994) Phytoplankton dynamics associated with a geostrophic front: ecological and biogeochemical implications. *J Mar Res* 52(4):711–742
- Cravo A, Relvas P, Cardeira S et al (2013) Nutrient and chlorophyll a transports during an upwelling event in the NW margin of the Gulf of Cadiz. *J Mar Syst* 128:208–221
- Crombet Y, Leblanc K, Quéguiner B et al (2011) Deep-silicon maxima in the stratified oligotrophic Mediterranean Sea. *Biogeosciences* 8:459–475
- D’Ortenzio F, Ribera d’Alcalà M (2009) On the trophic regimes of the Mediterranean Sea: a satellite analysis. *Biogeosciences* 6:139–148
- Dafner EV, Boscolo R, Bryden HL (2003) The N:Si:P molar ratio in the Strait of Gibraltar. *Geophys Res Lett* 30(10):1506. <https://doi.org/10.1029/2002GL016274>
- Denis-Karafistan A, Martin JM, Minas H et al (1998) Space and seasonal distributions of nitrates in the Mediterranean Sea derived from a variational inverse model. *Deep-Sea Res I* 45 (2–3):387–408
- Dubois C, Somot S, Calmanti S et al (2012) Future projections of the surface heat and water budgets of the Mediterranean Sea in an ensemble of coupled atmosphere–ocean regional climate models. *Clim Dyn* 39(7–8):1859–1884
- Duce RA, LaRoche J, Altieri K et al (2008) Impacts of atmospheric nitrogen on the open ocean. *Science* 320(5878):893–897
- Durrieu De Madron X, Guieu C, Sempere R et al (2011) Marine ecosystems responses to climatic and anthropogenic forcings in the Mediterranean. *Prog Oceanogr* 91(2):97–166
- Dutkiewicz S, Jeffrey Morris JJ, Follows MJ et al (2015) Impact of ocean acidification on the structure of future phytoplankton communities. *Nat Clim Change* 5:1002–1006
- Echevarría F, Lafuente JG, Bruno M et al (2002) Physical and biological coupling in the Strait of Gibraltar. *Deep-Sea Res II* 49:4115–4130
- Estrada M (1996) Primary production in the northwestern Mediterranean. *Sci Mar* 60(2):55–64
- Font J (1987) The path of the Levantine intermediate water to the Alboran sea. *Deep-Sea Res I* 34 (10):1745–1755
- García-Gorriz E, Carr ME (1999) The climatological annual cycle of satellite derived phytoplankton pigments in the Alboran Sea. *Geophys Res Lett* 26(19):2985–2988
- García-Gorriz E, Carr ME (2001) Physical control of phytoplankton distributions in the Alboran Sea: a numerical and satellite approach. *J Geophys Res* 106(16):795–805
- García-Martínez MC, Vargas-Yáñez M, Moya F et al (2017) The effects of climate change and rivers damming in the Mediterranean sea during the twentieth century. *Int J Environ Sci Nat Res* 8(4):555741. <https://doi.org/10.19080/IJESNR.2018.08.555741>
- García-Martínez MC, Vargas-Yáñez M, Moya F et al (2019) Average nutrient and chlorophyll distributions in the western Mediterranean: RADMED project. *Oceanologia* 61(1):143–169
- Gascard JC, Richez C (1985) Water masses and circulation in the western Alboran Sea and in the Straits of Gibraltar. *Prog Oceanogr* 15(3):157–216
- Gil J, Gomis D (1994) Circulación geostrofica, dinámica de mesoescala y fertilización de los niveles superficiales en el sector norte del mar de Alborán. Julio 1991. *Bol Inst Esp Oceanogr* 10 (1):95–117
- Giorgi F, Lionello P (2008) Climate change projections for the Mediterranean region. *Glob Planet Change* 63(2–3):90–104
- Gómez F, Gonzalez N, Echevarría F et al (2000) Distribution and fluxes of dissolved nutrients in the Strait of Gibraltar and its relationships to microphytoplankton biomass. *Estuar Coast Shelf S* 51 (4):439–449
- Gómez F, Gorsky G, Striby L et al (2001) Small-scale temporal variations in biogeochemical features in the Strait of Gibraltar, Mediterranean side—the role of NACW and the interface oscillation. *J Mar Syst* 30(3–4):207–220

- Gómez F, Gorsky G, García-Górriz E, Picheral M (2004) Control of the phytoplankton distribution in the Strait of Gibraltar by wind and fortnightly tides. *Estuar Coast Shelf S* 59(3):485–497
- Gomis D, Álvarez-Fanjul E, Jordà G et al (2016) Regional marine climate scenarios in the NE Atlantic sector close to the Spanish shores. *Sci Mar* 80(S1):215–234
- Goyet C, Hassoun AER, Gemayel E et al (2016) Thermodynamic Forecasts of the Mediterranean Sea Acidification. *Mediterranean Mar Sci* 17(2):508–518
- Gualdi S, Somot S, Li L et al (2013) The CIRCE simulations: regional climate change projections with realistic representation of the Mediterranean Sea. *Bull Am Meteorol Soc* 94(1):65–81
- Harzallah A, Jordà G, Dubois C et al (2018) Long term evolution of heat budget in the Mediterranean Sea from Med-CORDEX forced and coupled simulations. *Clim Dyn* 51(3):1145–1165
- Herrmann M, Diaz F, Estournel C et al (2013) Impact of atmospheric and oceanic interannual variability on the Northwestern Mediterranean Sea pelagic planktonic ecosystem and associated carbon cycle. *J Geophys Res Oceans* 118(10):5792–5813
- Herrmann M, Estournel C, Adloff F et al (2014) Impact of climate change on the northwestern Mediterranean Sea pelagic planktonic ecosystem and associated carbon cycle. *J Geophys Res Oceans* 119(9):5815–5836
- Howarth RW (1988) Nutrient limitation of net primary production in marine ecosystems. *Annu Rev Ecol Evol S* 19:89–110
- Huertas IE, Ríos AF, García-Lafuente J et al (2012) Atlantic forcing of the Mediterranean oligotrophy. *Global Biogeochem Cy* 26:GB2022. <https://doi.org/10.1029/2011GB004167>
- Incarbona A, Martrat B, Mortyn PG et al (2016) Mediterranean circulation perturbations over the last five centuries: relevance to past Eastern Mediterranean Transient-type events. *Sci Rep* 6:29623. <https://doi.org/10.1038/srep29623>
- IPCC (2007) Climate change 2007: the physical science basis Contribution of working group I to the fourth assessment report of the intergovernmental panel on climate change. Cambridge University Press, Cambridge
- IPCC (2013) Climate Change 2013: The Physical Science Basis Contribution of Working Group I to the Fifth Assessment Report of the Intergovernmental Panel on Climate Change. In: Stocker TF, Qin D, Plattner GK et al (eds) . Cambridge University Press, Cambridge
- Jacquet S, Prieur L, Avois-Jacquet C et al (2002) Short-timescale variability of picophytoplankton abundance and cellular parameters in surface waters of the Alboran Sea (western Mediterranean). *J Plank Res* 24(7):635–651
- Jordà G, Álvarez-Fanjul E, Aznar R et al (2011) The VANIMEDAT-2 project: generation of oceanographic scenarios for the 21st century for the Mediterranean Sea and the NE sector of the Atlantic Ocean. Paper presented at the WCRP OSC Conference (World Climate Research Programme). Climate Research in Service to Society, Denver, CO, 24–28 October 2011
- Karafistan A, Martin JM, Rixen M et al (2002) Space and time distributions of phosphate in the Mediterranean Sea. *Deep-Sea Res I* 49(1):67–82
- Kersting DK (2016) Cambio climático en el medio marino español: impactos, vulnerabilidad y adaptación Oficina Española de Cambio Climático, Ministerio de Agricultura, Alimentación y Medio Ambiente, Madrid, p 166
- Krom MD, Kress N, Brenner S (1991) Phosphorus limitation of primary productivity in the eastern Mediterranean Sea. *Limnol Oceanogr* 36(3):424–432
- L’Helguen S, Le Corre P, Madec C et al (2002) New and regenerated production in the Almeria-Oran front area, eastern Alboran Sea. *Deep-Sea Res I* 49(1):83–99
- Lafuente JG, Cano N, Vargas M et al (1998) Evolution of the Alboran Sea hydrographic structures during July 1993. *Deep-Sea Res I* 45(1):39–65
- Lafuente JG, Sarhan T, Vargas M et al (1999) Tidal motions and tidally induced fluxes through La Línea submarine canyon, western Alboran Sea. *J Geophys Res* 104(C2):3109–3119
- Lavigne H, D’Ortenzio F, Ribera D’Alcala M et al (2015) On the vertical distribution of the chlorophyll-a concentration in the Mediterranean sea: a basin scale and seasonal approach. *Biogeosciences* 12(16):5021–5039

- Lazzari P, Solidoro C, Ibello V et al (2012) Seasonal and inter-annual variability of plankton chlorophyll and primary production in the Mediterranean Sea: a modelling approach. *Biogeosciences* 9(1):217–233
- Lazzari P, Mattia G, Solidoro C et al (2014) The impacts of climate change and environmental management policies on the trophic regimes in the Mediterranean Sea: a scenario analysis. *J Mar Syst* 135:137–149
- Lazzari P, Solidoro C, Salon S et al (2016) Spatial variability of phosphate and nitrate in the Mediterranean Sea: a modeling approach. *Deep-Sea Res I* 108:39–52
- Leblanc K, Quéguiner B, Prieur L et al (2004) Siliceous phytoplankton production and export related to trans-frontal dynamics of the Almeria-Oran frontal system (western Mediterranean Sea) during winter. *J Geophys Res* 109:C07010. <https://doi.org/10.1029/2003JC001878>
- Lejeune C, Chevaldonné P, Pergent-Martini C et al (2010) Climate change effects on a miniature ocean: the highly diverse, highly impacted Mediterranean Sea. *Trends Ecol Evol* 25:250–260
- Lionello P, Gacic M, Gomis D et al (2010) Program focuses on climate of the Mediterranean region. *Eos Trans AGU* 93(10):105–106
- Lohrenz SE, Wiesenburg DA, De Palma IP et al (1988) Interrelationships among primary production, chlorophyll and environmental conditions in frontal regions of the western Mediterranean Sea. *Deep-Sea Res* 35(5):793–810
- Macías D, Navarro G, Echevarría F et al (2007) Phytoplankton pigment distribution in the north-western Alboran Sea and meteorological forcing: a remote sensing study. *J Mar Res* 65(4):523–543
- Macías D, Bruno M, Echevarría F et al (2008) Meteorologically-induced mesoscale variability of the North-western Alboran Sea (southern Spain) and related biological patterns. *Estuar Coast Shelf S* 78(2):250–266
- Macías D, Navarro G, Bartual A et al (2009) Primary production in the Strait of Gibraltar: carbon fixation rates in relation to hydrodynamic and phytoplankton dynamics. *Estuar Coast Shelf S* 83(2):197–210
- Macías D, Castilla-Espino D, García del Hoyo J et al (2014a) Consequences of a future climatic scenario for the anchovy fishery in the Alboran Sea (SW Mediterranean): a modelling study. *J Mar Syst* 135:150–159
- Macías D, Garcia-Gorriz E, Piroddi C et al (2014b) A Biogeochemical control of marine productivity in the Mediterranean Sea during the last 50 years. *Global Biogeochem Cy* 28:897–907
- Macías D, Garcia-Gorriz E, Stips A (2015) Productivity changes in the Mediterranean Sea for the twenty-first century in response to changes in the regional atmospheric forcing. *Front Mar Sci* 2:79. <https://doi.org/10.3389/fmars.2015.00079>
- Macías D, Stips A, Garcia-Gorriz E et al (2018) Hydrological and biogeochemical response of the Mediterranean Sea to freshwater flow changes for the end of the 21st century. *PLoS ONE* 13(2): e0192174. <https://doi.org/10.1371/journal.pone.0192174>
- MacIsaac JJ, Dugdale RC (1969) The kinetics of nitrate and ammonia uptake by natural populations of marine phytoplankton. *Deep Sea Res* 16(1):47–58
- Manca B, Burca M, Giorgetti A et al (2004) Physical and biochemical averaged vertical profiles in the Mediterranean regions: an important tool to trace the climatology of water masses and to validate incoming data from operational oceanography. *J Mar Syst* 48(1–4):83–116
- Mariotti A, Zeng N, Yoon JH et al (2008) Mediterranean water cycle changes: transition to drier 21st century conditions in observations and CMIP3 simulations. *Environ Res Lett* 3(4):044001. <https://doi.org/10.1088/1748-9326/3/4/044001>
- Mariotti A, Pan Y, Zeng N et al (2015) Long-term climate change in the Mediterranean region in the midst of decadal variability. *Clim Dyn* 44(5–6):1437–1456
- Meier KJS, Beaufort L, Heussner S et al (2014) The role of ocean acidification in *Emiliania huxleyi* coccolith thinning in the Mediterranean Sea. *Biogeosciences* 11:2857–2869
- Mercado JM, Ramírez T, Cortés D et al (2005) Temporal changes of the phytoplankton communities in an upwelling area of the Alborán Sea. *Sci Mar* 69(4):451–465

- Mercado JM, Cortés D, García A et al (2007) Seasonal and inter-annual changes in the planktonic communities of the northwest Alboran Sea (Mediterranean Sea). *Prog Oceanogr* 74 (2–3):273–293
- Mercado JM, Ramírez T, Cortés D et al (2008) Partitioning the effects of changes in nitrate availability and phytoplankton community structure on relative nitrate uptake. *Mar Ecol Prog Ser* 359:51–68
- Mercado JM, Cortes D, Ramirez T et al (2012) Decadal weakening of the wind-induced upwelling reduces the impact of nutrient pollution in the Bay of Málaga (western Mediterranean Sea). *Hydrobiologia* 680(1):91–107
- Mercado JM, Sala I, Salles S et al (2014) Effects of community composition and size structure on light absorption and nutrient uptake of phytoplankton in contrasting areas of the Alboran Sea. *Mar Ecol Prog Ser* 499:47–64
- Millot C (1999) Circulation in the western Mediterranean Sea. *J Mar Syst* 20(1–4):423–442
- Minas HJ, Coste B, Le Corre P et al (1991) Biological and geochemical signatures associated with the water circulation through the Strait of Gibraltar and in the western Alboran Sea. *J Geophys Res* 96(C5):8755–8771
- Morán XAG, Estrada M (2001) Short-term variability of photosynthetic parameters and particulate and dissolved primary production in the Alboran sea (SW Mediterranean). *Mar Ecol Prog Ser* 212:53–67
- Morel A, Andre JM (1991) Pigment distribution and primary production in the western Mediterranean as derived and modelled from Coastal Zone Color Scanner observations. *J Geophys Res* 96(C7):12685–12698
- Moutin T, Raimbault P (2002) Primary production, carbon export and nutrients availability in western and eastern Mediterranean Sea in early summer 1996 (MINOS cruise). *J Mar Syst* 33-34:273–288
- Muñoz M, Reul A, Vargas-Yáñez M et al (2017) Fertilization and connectivity in the Garrucha Canyon (SE-Spain) implications for Marine Spatial Planning. *Mar Environ Res* 126:45–68
- Nakicenovic N, Swart R (eds) (2000) Special Report on Emissions Scenarios. A Special Report of Working Group III of the Intergovernmental Panel on Climate Change. Cambridge University Press, Cambridge
- Navarro G, Vazquez A, Macías D et al (2011) Understanding the patterns of biological response to physical forcing in the Alboran Sea (western Mediterranean). *Geophys Res Lett* 38:L23606. <https://doi.org/10.1029/2011GL049708>
- Nelson DM, Dortch Q (1996) Silicic acid depletion and silicon limitation in the plume of the Mississippi River: evidence from kinetic studies in spring and summer. *Mar Ecol Prog Ser* 136:163–178
- Oguz T, Macias D, Garcia-Lafuente J et al (2014) Fueling plankton production by a meandering frontal jet: a case study for the Alboran Sea (Western Mediterranean). *PLoS One* 9(11):e111482. <https://doi.org/10.1371/journal.pone.0111482>
- Orr J, Fabry V, Aumont O et al (2005) Anthropogenic ocean acidification over the twenty first century and its impact on calcifying organisms. *Nature* 437:681–686
- Packard TT, Minas HJ, Costé B et al (1988) Formation of the Alboran oxygen minimum zone. *Deep-Sea Res* 35(7):1111–1118
- Padorno E, Aznar R, Álvarez-Fanjul E et al (2012) Impact of climate change scenarios in the Mediterranean Sea from a regional ocean model. *Geophys Res Abst* 14:EGU2012-8932
- Parrilla G, Kinder TH (1987) Oceanografía física del mar de Alborán. *Bol Inst Esp Oceanogr* 4:133–165
- Parrilla G, Kinder TH, Preller R (1986) Deep and intermediate Mediterranean Water in the western Alboran Sea. *Deep-Sea Res* 33(1):55–88
- Pasqueron de Fommervault O (2015) Dynamique des nutriments en Méditerranée : des campagnes océanographiques aux flotteurs Bio-Argo. *Océanographie. Thèse de doctorat. Océanographie. Université Pierre et Marie Curie, Paris VI*

- Perkins H, Kinder T, La Violette PE (1990) The Atlantic inflow in the Western Alboran Sea. *J Phys Oceanogr* 20(2):242–263
- Pinot JM, Ganachaud A (1999) The role of Winter Intermediate Water in the spring-summer circulation of the Balearic Sea. Part 1. Hydrography and inverse modelling. *J Geophys Res* 104(C12):29843–29864
- Pinot JM, López-Jurado J, Riera M (2002) The Canales experiment (1996–1998). Interannual, seasonal and mesoscale variability of the circulation in the Balearic channels. *Prog Oceanogr* 55 (3–4):335–370
- Powley HR, Krom MD, Van Cappellen P (2018) Phosphorus and nitrogen trajectories in the Mediterranean Sea (1950–2030): understanding basin-wide anthropogenic nutrient enrichment. *Progr Oceanogr* 162:257–270
- Prieto L, García CM, Corzo A et al (1999) Phytoplankton, bacterioplankton and nitrate reductase activity distribution in relation to physical structure in the northern Alboran Sea and Gula of Cádiz (southern Iberian Peninsula). *Bol Inst Esp Oceanogr* 15(1–4):401–411
- Priour L, Sournia A (1994) “Almofront-1” (April–May 1991): an interdisciplinary study of the Almeria-Oran geostrophic front, SW Mediterranean Sea. *J Mar Syst* 5(3–5):187–203
- Ramírez T (2007) Variabilidad hidrológica y dinámica biogeoquímica en el sector noroccidental del mar de Alborán. Universidad de Málaga, Tesis Doctoral
- Ramírez T, Cortés D, Mercado JM et al (2005) Seasonal dynamics of inorganic nutrients and phytoplankton biomass in the NW Alboran Sea. *Estuar Coast Shelf S* 65(4):654–670
- Ramírez T, Liger E, Mercado JM et al (2006) Respiratory ETS activity of plankton in the northwestern Alboran Sea: seasonal variability and relationship with hydrological and biological features. *J Plankton Res* 28(7):629–641
- Ramírez-Romero E, Macías D, García CM et al (2014) Biogeochemical patterns in the Atlantic Inflow through the Strait of Gibraltar. *Deep-Sea Res I* 85:88–100
- Redfield AC, Ketchum BH, Richards FA (1963) The influence of organisms on the composition of sea-water. In: Hill MN (ed) *The sea*, vol 2. Wiley, New York, pp 26–77
- Reid PC, Fischer AC, Lewis-Brown E et al (2009) Impacts of the oceans on climate change. In: Sims DW (ed) *Advances in marine biology*, vol 56. Elsevier, pp 1–156
- Renault L, Oguz T, Pascual A et al (2012) Surface circulation in the Alborán Sea (western Mediterranean) inferred from remotely sensed data. *J Geophys Res* 117:C08009. <https://doi.org/10.3354/ab00585>
- Reul A, Rodríguez V, Jiménez-Gómez F et al (2005) Variability in the spatio-temporal distribution and size-structure of phytoplankton across an upwelling area in the NW-Alboran Sea, (W-Mediterranean). *Cont Shelf Res* 25(5–6):589–608
- Reul A, Muñoz M, Bautista B et al (2014) Effect of CO<sub>2</sub>, nutrients and light on coastal plankton III Trophic cascade, size structure and composition. *Aquat Biol* 22:59–76
- Ribera d’Alcalà M, Civitarese G, Conversano F et al (2003) Nutrient ratios and fluxes hint at overlooked processes in the Mediterranean. *J Geophys Res* 108(C9):8106. <https://doi.org/10.1029/2002JC001650>
- Richon C, Dutay JC, Dulac F et al (2018) Modeling the biogeochemical impact of atmospheric phosphate deposition from desert dust and combustion sources to the Mediterranean Sea. *Biogeosciences* 15(8):2499–2524
- Rodríguez J, Blanco JM, Jiménez-Gómez F et al (1998) Patterns in the size structure of the phytoplankton community in the deep fluorescence maximum of the Alboran Sea (southwestern Mediterranean). *Deep-Sea Res I* 45:1577–1593
- Roether W, Klein B, Manca BB et al (2007) Transient Eastern Mediterranean deep waters in response to massive dense-water output of the Aegean Sea in the 1990s. *Progr Oceanogr* 74 (4):540–571
- Roether W, Klein B, Hainbucher D (2014) The Eastern Mediterranean Transient. Evidence for similar events previously? In: Borzelli GL, Gačić M, Lionello P et al (eds) *The Mediterranean Sea: temporal variability and spatial patterns*. Geophysical monograph series, vol 202. Wiley, New York, pp 75–83

- Rubín JP, Gil J, Ruiz J et al (1992) La distribución ictioplactónica y su relación con los parámetros físicos, químicos y biológicos en el sector norte del mar de Alborán, en julio de 1991 (resultados de la campaña Ictioalborán 0791). *Inf Téc Inst Esp Oceanogr* 139:3–49
- Rubín JP, Cano N, Arrate P et al (1997) El ictioplancton el mesozooplancton y la hidrología en el Golfo de Cádiz, Estrecho de Gibraltar y sector noroeste del mar de Alborán, en julio de 1994. *Inf Téc Inst Esp Oceanogr* 167:3–44
- Rubín JP, Cano N, Prieto L et al (1999) La estructura del ecosistema pelágico en relación las condiciones oceanográficas en el Golfo de Cádiz, Estrecho de Gibraltar y mar de Alborán (sector noroeste), en julio de 1995. *Inf Téc Inst Esp Oceanogr* 175:3–73
- Ruiz J, Echevarría F, Font J et al (2001) Surface distribution of chlorophyll, particles and gelbstoff in the Atlantic jet of the Alborán Sea: from submesoscale to subinertial scales of variability. *J Mar Syst* 29(1–4):277–292
- Ruti P, Somot S, Giorgi F et al (2016) Med-CORDEX initiative for Mediterranean climate studies. *Bull Am Meteorol Soc* 97(7):1187–1208
- Sabine CL, Feely RA, Gruber N et al (2004) The oceanic sink for anthropogenic CO<sub>2</sub>. *Science* 305(5682):367–371
- Salat J, Font J (1987) Water mass structure near and offshore the Catalan coast during winters 1982 and 1983. *Ann Geophys* 5B(1):49–54
- Sanchez-Gomez E, Somot S, Josey SA et al (2011) Evaluation of Mediterranean Sea water and heat budgets simulated by an ensemble of high resolution regional climate models. *Clim Dyn* 37:2067–2086
- Sánchez-Vidal A, Calafat A, Canals M et al (2004) Particle flux in the Almeria-Oran front: control by coastal upwelling and sea-surface circulation. *J Mar Syst* 52(1–4):89–106
- Sarhan T, García Lafuente J, Vargas-Yáñez M et al (2000) Upwelling mechanisms in the north-western Alboran Sea. *J Mar Syst* 23(4):317–331
- Sarmiento JL, Gruber N, Brzezinski MA et al (2004) High latitude controls of thermocline nutrients and low latitude biological productivity. *Nature* 427:56–60
- Schroeder K, García-Lafuente J, Josey S et al (2012) Circulation of the Mediterranean Sea and its variability. In: Lionello P (ed) *The Mediterranean climate: from the past to the future*. Elsevier, London, pp 187–256
- Schroeder K, Chiggiato J, Josey SA et al (2017) Rapid response to climate change in a marginal sea. *Sci Rep* 7:4065. <https://doi.org/10.1038/s41598-017-04455-5>
- Semperé R, Dafner E, Van Wambeke F et al (2003) Distribution and cycling of total organic carbon across the Almeria-Oran Front in the Mediterranean Sea: implications for carbon cycling in the western basin. *J Geophys Res* 108(11):3361. <https://doi.org/10.1029/2002JC001475>
- Sevault F, Somot S, Alias A et al (2014) A fully coupled Mediterranean regional climate system model: design and evaluation of the ocean component for the 1980–2012 period. *Tellus A* 66(1):23967. <https://doi.org/10.3402/tellusa.v66.23967>
- Snaith HM, Alderson SG, Allen JT et al (2003) Monitoring the eastern Alborán Sea using combined altimetry and in situ data. *Philos Trans A Math Phys Eng Sci* 361:65–70
- Somot S, Sevault F, Déqué M (2006) Transient climate change scenario simulation of the Mediterranean Sea for the twenty-first century using a high-resolution ocean circulation model. *Clim Dyn* 27(7–8):851–879
- Somot S, Sevault F, Déqué M et al (2008) 21st century climate change scenario for the Mediterranean using a coupled atmosphere–ocean regional climate model. *Glob Planet Change* 63(2–3):112–126
- Soto-Navarro J, Somot S, Sevault F et al (2015) Evaluation of regional ocean circulation models for the Mediterranean Sea at the Strait of Gibraltar: volume transport and thermohaline properties of the outflow. *Clim Dyn* 44(5–6):1–16
- Sournia A (1973) La production primaire planctonique en Méditerranée: Essai de mise à jour. *Bulletin de l'Étude en commun de la Méditerranée* 5:1–128
- Spalding MD, Fox HE, Allen GR et al (2007) Marine ecoregions of the world: a bioregionalization of coastal and shelf areas. *BioScience* 57(7):573–583

- Stambler N (2014) The Mediterranean Sea – primary productivity. In: Goffredo S, Dubinsky Z (eds) *The Mediterranean Sea*. Springer, Dordrecht
- Stanichny S, Tigny V, Stanichnaya R et al (2005) Wind driven upwelling along the African coast of the Strait of Gibraltar. *Geophys Res Lett* 32:L04604. <https://doi.org/10.1029/2004GL021760>
- Steinacher M, Joos F, Frölicher TL et al (2010) Projected 21st century decrease in marine productivity: a multi-model analysis. *Biogeosciences* 7:979–1005
- Taucher J, Oschlies A (2011) Can we predict the direction of marine primary production change under global warming? *Geophys Res Lett* 38:L02603. <https://doi.org/10.1029/2010GL045934>
- Teruzzi A, Cossarini G, Lazzari P, Salon S, Bolzon G, Crise A, Solidoro C (2016) Mediterranean Sea biogeochemical reanalysis (CMEMS MED REA-Biogeochemistry 1999–2015). [Data set]. Copernicus Monitoring Environment Marine Service. [https://doi.org/10.25423/MEDSEA\\_REANALYSIS\\_BIO\\_006\\_008](https://doi.org/10.25423/MEDSEA_REANALYSIS_BIO_006_008)
- Thingstad TF, Zweifel UL, Rassoulzadegan F (1998) P limitation of heterotrophic bacteria and phytoplankton in the northwest Mediterranean. *Limnol Oceanogr* 43(1):88–94
- Thingstad TF, Krom MD, Mantoura RFC et al (2005) Nature of phosphorus limitation in the ultraoligotrophic Eastern Mediterranean. *Science* 309(5737):1068–1071
- Thorpe RB, Bigg GR (2000) Modelling the sensitivity of Mediterranean outflow to anthropogenically forced climate change. *Clim Dyn* 16(5):355–368
- Tintore J, La Violette PE, Blade I, Cruzado A (1988) A study of an intense density front in the eastern Alboran Sea: the Almeria-Oran front. *J Phys Oceanogr* 18(19):1384–1397
- Tintoré J, Gomis D, Alonso S et al (1991) Mesoscale dynamics and vertical motion in the Alboran Sea. *J Phys Oceanogr* 21(6):811–823
- Tsimplis MN, Zervakis V, Josey SA et al (2006) Chapter 4 Changes in the oceanography of the Mediterranean Sea and their link to climate variability. In: Lionello P, Malanotte-Rizzoli P, Boscolo R (eds) *Mediterranean*. p 227–282
- Turley CM (1999) The changing Mediterranean Sea sensitive ecosystem? *Prog Oceanogr* 44(1–3):387–400
- Van Haren H (2014) Internal wave–zooplankton interactions in the Alboran Sea (W-Mediterranean). *J Plank Res* 36(4):1124–1134
- Vargas-Yañez M, Plaza F, García-Lafuente J et al (2002) About the seasonal variability of the Alboran Sea circulation. *J Mar Syst* 35(3–4):229–248
- Vargas-Yañez M, García MJ, Salat J et al (2008) Warming trends and decadal variability in the Western Mediterranean shelf. *Glob Planet Change* 63(2–3):177–184
- Vargas-Yañez M, Zunino P, Schroeder K et al (2012) Extreme Western Intermediate Water formation in Winter 2010. *J Mar Syst* 105–108:52–29
- Vázquez A, Bruno M, Izquierdo A et al (2008) Meteorologically forced subinertial flows and internal wave generation at the main Sill of the Strait of Gibraltar. *Deep-Sea Res I* 55(10):1277–1283
- Vázquez A, Flecha S, Bruno M et al (2009) Internal waves and short-scale distribution patterns of chlorophyll in the Strait of Gibraltar and Alborán Sea. *Geophys Res Lett* 36:L23601. <https://doi.org/10.1029/2009GL040959>
- Vélez-Belchí P, Vargas-Yañez M, Tintoré J (2005) Observation of a western Alborán gyre migration event. *Prog Oceanogr* 66(2–4):190–210
- Viúdez A, Tintoré J, Haney RL (1996) Circulation in the Alboran Sea as determined by quasisyntropic hydrographic observations. Part I: Three-dimensional structure of the two anticyclonic gyres. *J Phys Oceanogr* 26(5):684–705
- Waldman R, Somot S, Herrmann M et al (2017) Modeling the intense 2012–2013 dense water formation event in the northwestern Mediterranean Sea: Evaluation with an ensemble simulation approach. *J Geophys Res Oceans* 122:1297–1324